



Recent Advances in Incoherent and Coherent OTR Diagnostics

R. B. Fiorito

Institute for Research in Electronics and Applied Physics
University of Maryland, College Park , MD

PAC09, May 3-8, 2009, Vancouver, BC

Outline of Talk*

- 1) Explanation of TR and OTR
- 2) Incoherent OTR Properties and Applications
- 3) Coherent TR, OTR Properties
- 4) COTR Observations for Long pulses ($ct \gg \lambda$) and Interpretation
- 5) Mitigation of COTR
- 6) Simulation Code predictions using ELEGANT

*Special thanks for assistance in preparing this talk to

- A. Shkvarunets (UMD)
- H. Loos, Z. Huang (SLAC)
- F. Sannibale (LBNL)
- A. Lumpkin (FNAL)
- C. Welsche (U Liverpool)

AND ALL MY COLLEAGUES!

Transition Radiation in a Nutshell

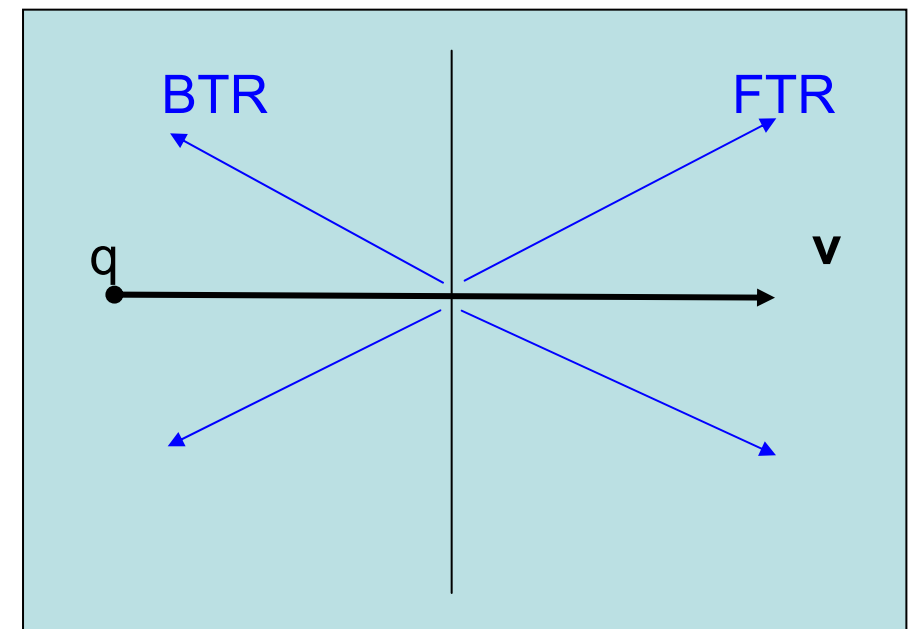
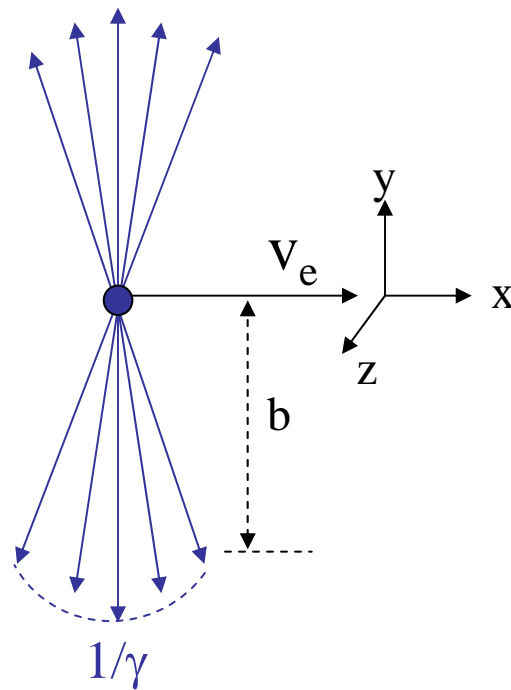
Definition:

Radiation which occurs when charge moving at constant velocity crosses a boundary between media with different dielectric constants

Weissacker-Williams

(virtual photon picture) Reflection and refraction of virtual photons of all frequencies (up to plasma frequency) at the interface

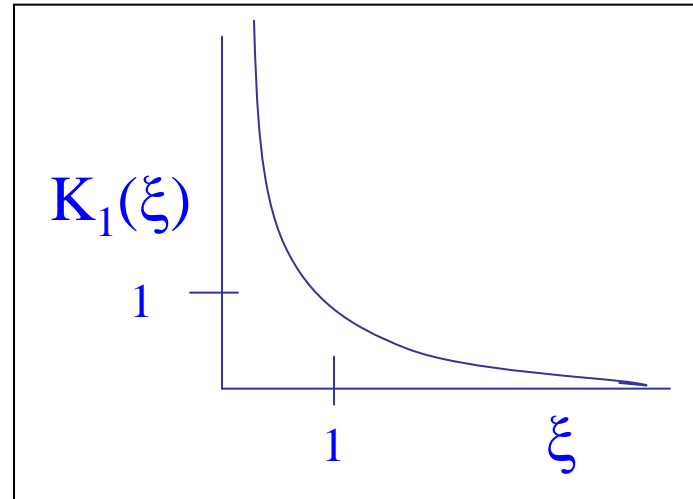
What is really radiating? the image charge current (Important to remember)



Fourier Spectrum of Virtual Photon Pulse

Fourier components are transverse plane waves with spectrum:

$$\hat{E}(\omega) = \frac{q}{\pi} \frac{\omega}{\gamma c} K_1 \left(\frac{\omega r}{\gamma c} \right)$$



b is the **radiation impact parameter** which represents the effective spatial extent and source size, $b = \gamma\lambda/2\pi$ of the virtual photon with wave number $\kappa = \omega/c$.

Properties of Incoherent Transition Radiation ($\lambda \ll ct_b$) useful for beam diagnostics

1. Prompt : fs response time
2. Broad band: flat frequency spectrum up to plasma freq. of radiator material
3. Intensity linear with charge $I \sim N$
4. Angular distribution peaks at $1/\gamma$
5. Polarized in direction of radiation lobes (radial polarization)
6. Beamed in direction of velocity of charge(relativistic)
4. OTR: High spatial resolution for imaging (independent of particle energy)
ultimate resolution: point spread function determined by field of charge and angular acceptance of optics
5. Low photon yield per electron ~ 0.001- 0.001 in visible band

Diagnostics of beam parameters using IOTR

1-Near Field Imaging (spatial distribution)

size (x, y)

position (x, y) (offset)

2-Far Field Imaging (angular distribution)

divergence (x', y') [angular resolution < $0.01/\gamma$]

trajectory angle (X',Y') [$<0.01/\gamma$]

energy (average) and energy spread [<0.01]

3- Spectrum : fluctuations can be used to measure bunch length (proven using Incoh. OSR)

Point Spread Function of OTR for Imaging determined field of charge and angular acceptance of Lens

For $\Theta = d / l \gg 1/\gamma$

$$E_{PSF} \sim (\gamma\lambda)^{-1} K_1(r/(\gamma\lambda)) - r^{-1} J_0(r\Theta/\lambda)$$

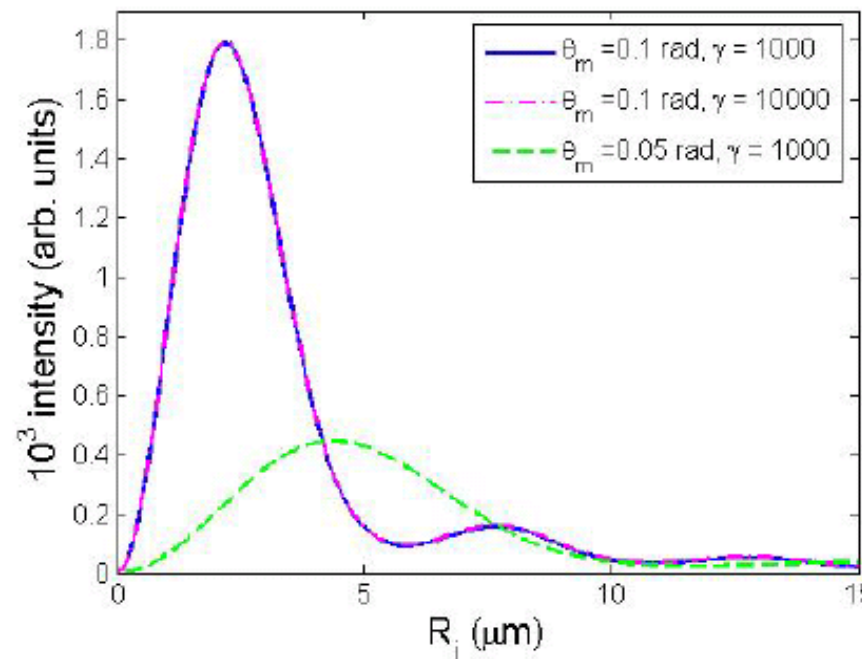
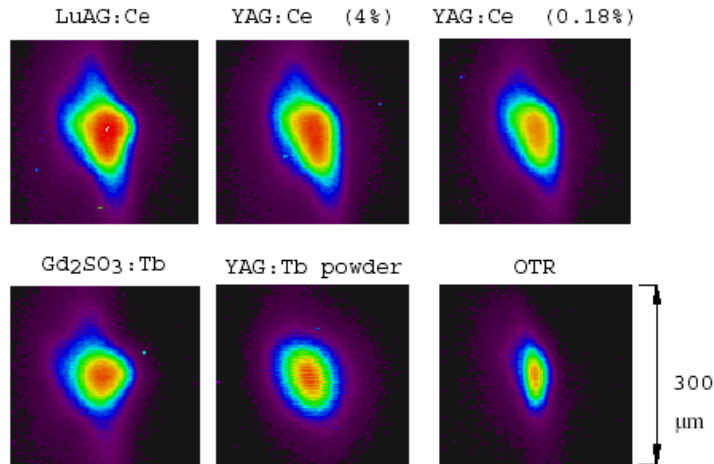


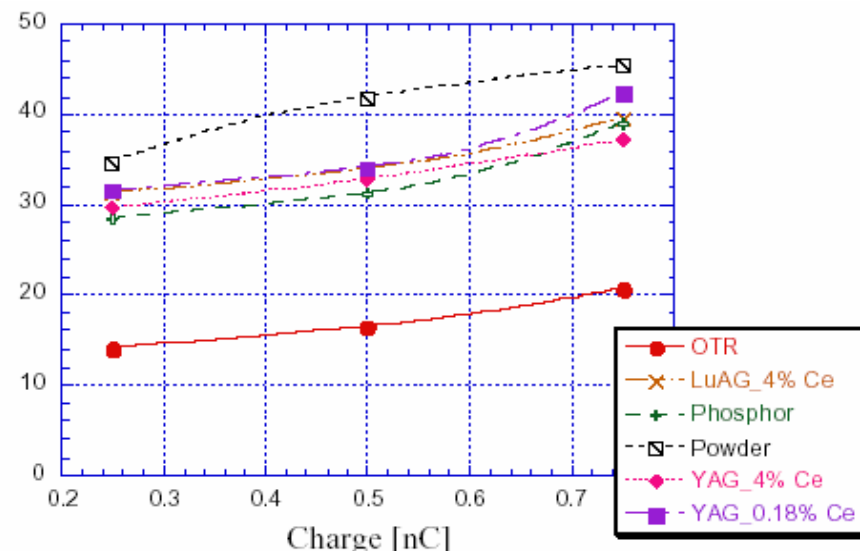
FIG. 2 (Color) PSF of the OTR for various beam energies and various lens acceptance angles.

*D. Xiang, et. al. PRSTAB (2007)

Comparison of Imaging Screens YAG, Phosphor, OTR



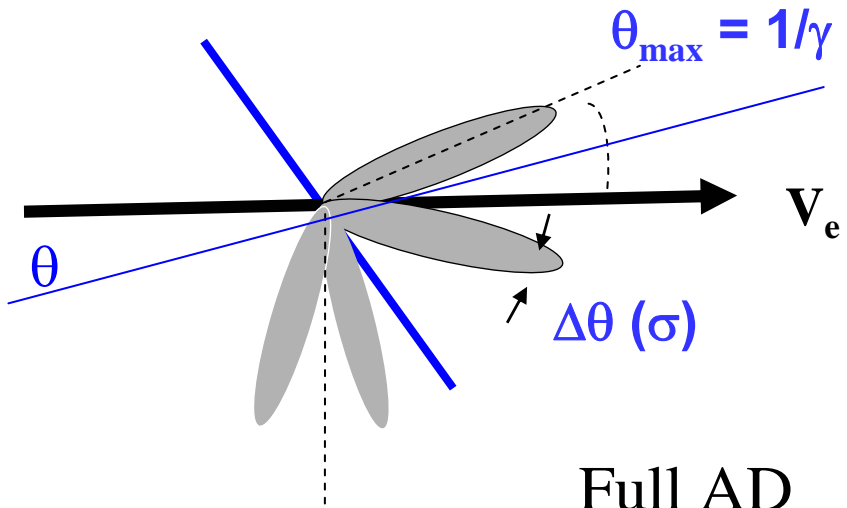
Resolution: Beam images taken with six different diagnostic screens under the stable experimental conditions ($Q \sim 500$ pC) at the **ATF/BNL 40 MeV linac** by Yakimenko, et. al.



Linearity : Electron beam horizontal spot size as a function of charge, measured with scintillating diagnostics and OTR (sub micron resolution independent of energy).

IOTR Angular Distribution: Beam Trajectory Angle and Divergence

{ independent of frequency and beam size (or position) }

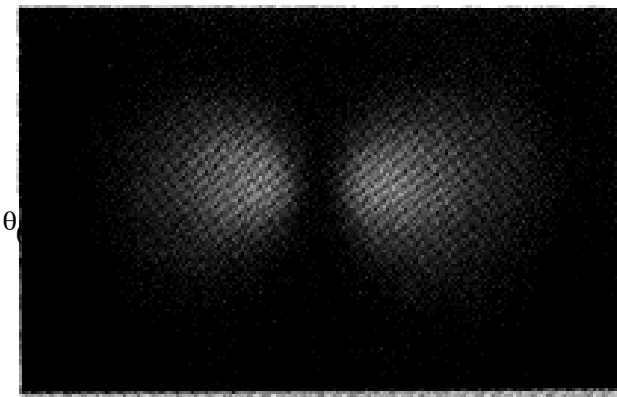
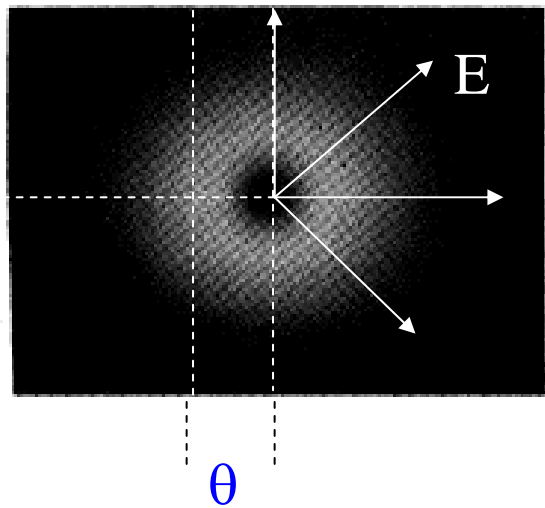


Full AD

$$\frac{d^2I^{(S)}}{d\omega d\Omega} = |r_{\square, \perp}|^2 \frac{e^2}{\pi^2 c} \frac{\theta^2}{(\gamma^{-2} + \theta^2)^2},$$
$$\theta \gg \gamma^{-1} \gg 1$$

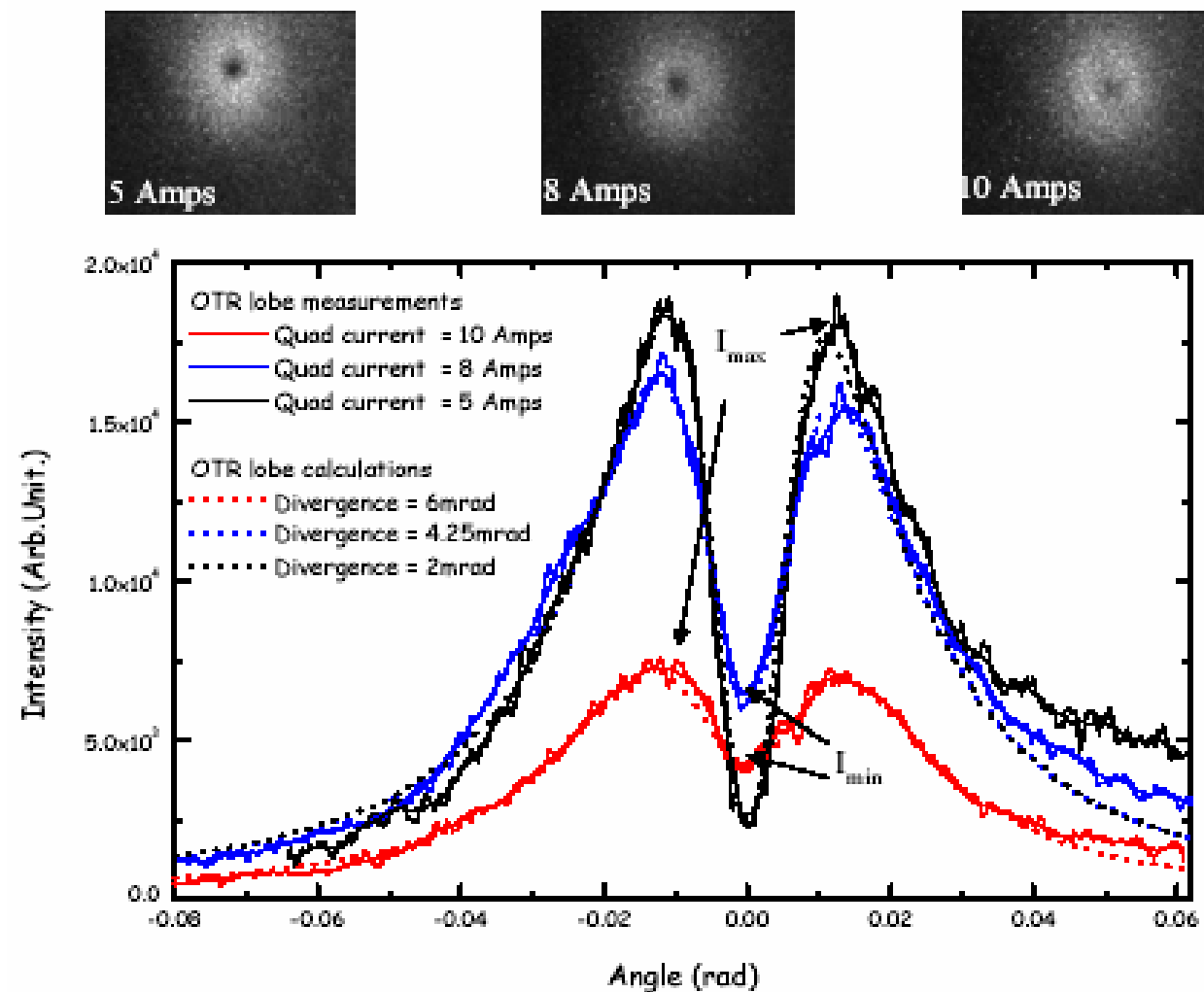
Horizontally Polarized AD

Radially
Polarized
AD Pattern
Centered on
Direction of
 V_e



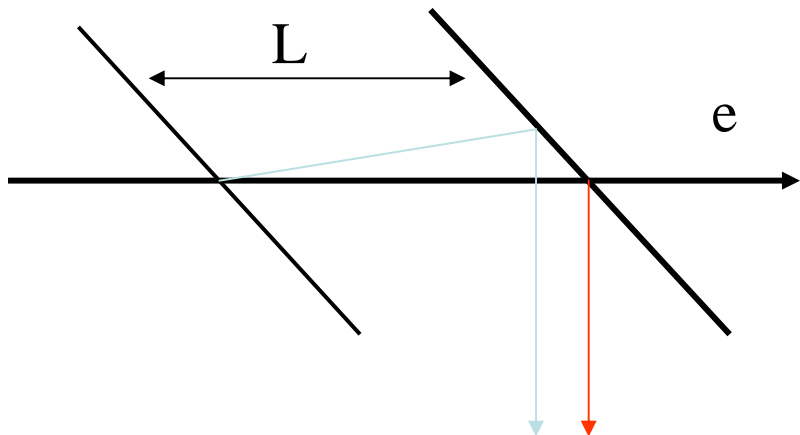
Effect of Divergence on OTR Angular Distribution and Horizontal Scans

(48 MeV CLIC2 Test Facility Beam)



IOTR Interferometry provides greater sensitivity to beam parameters

Two Foil OTRI

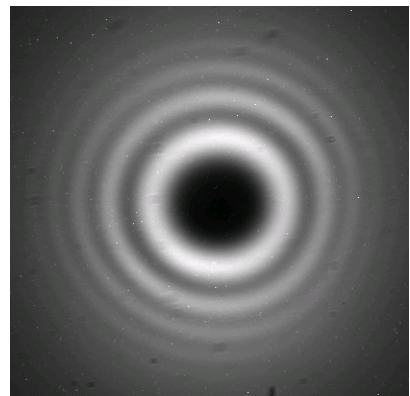


$$\frac{d^2I_{TOT}}{d\omega d\Omega} = \left[\frac{e^2}{\pi^2 c} \frac{\theta^2}{(\gamma^{-2} + \theta^2)^2} \right] |1 - e^{-i\phi}|^2,$$

where : $\phi = L / L_v$,

$$L_v = (\lambda / \pi)(\gamma^{-2} + \theta^2)^{-1}$$

(vacuum coherence length)



θ_x

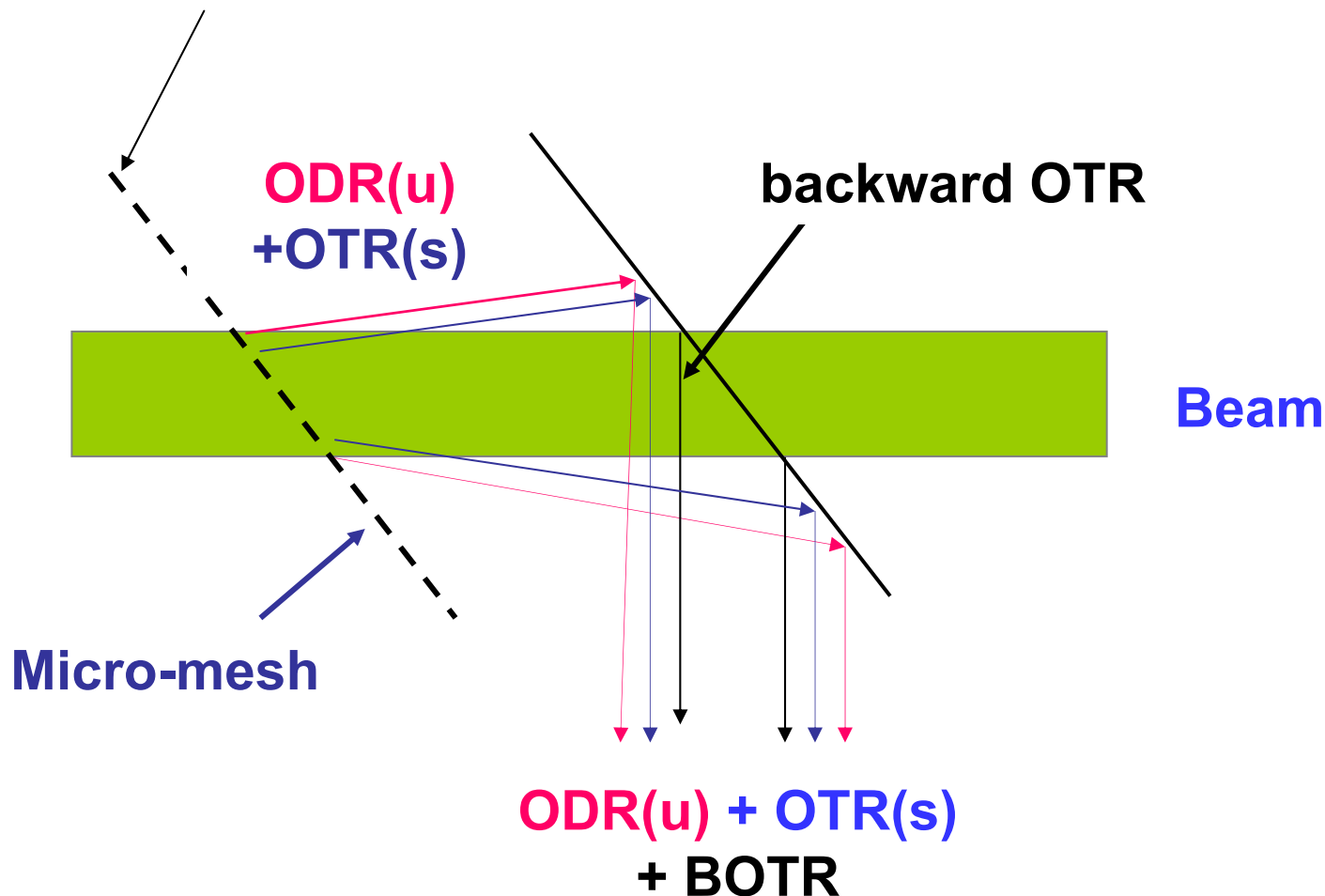
θ_y

- Center of pattern measures trajectory angle of particle
- Visibility of OTRI measures beam divergence (and/or $\Delta E/E$)
- Radial Polarization of OTRI can be used to *separately* measure x' and y'
- *Fringe position measures beam energy (E)*

Optical Diffraction-Transition Radiation Interferometry

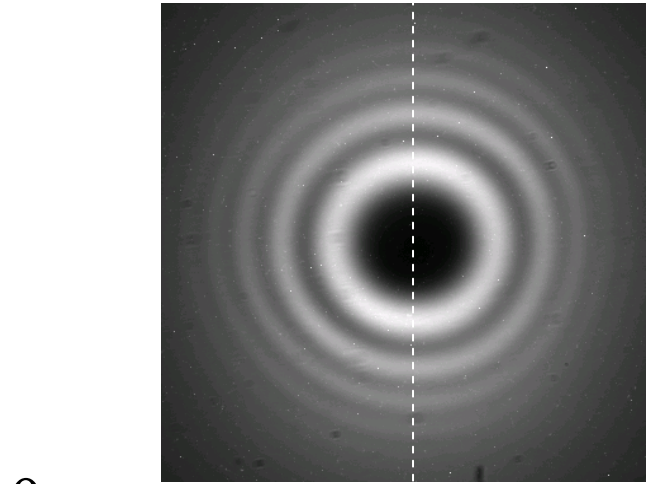
Extends OTRI diagnostics to low energy and/or low emittance beams

Micro-mesh front foil overcomes scattering limit of conventional OTRI

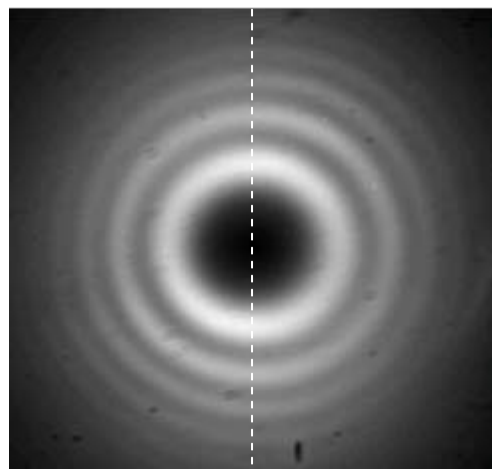


Comparison of OTR and ODTR Interferograms

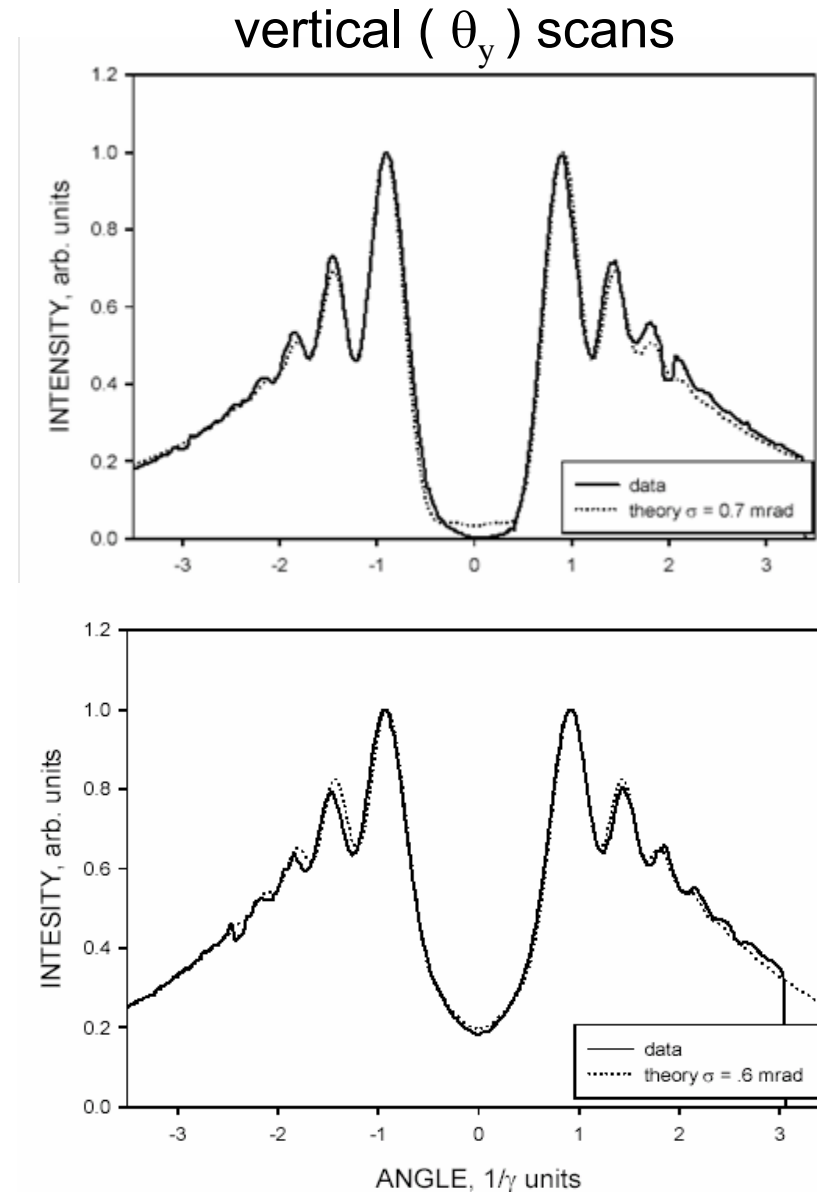
Vertical (y) beam waist, $E = 95$ MeV (NPS linac), $\lambda = 650 \times 70$ nm



OTRI

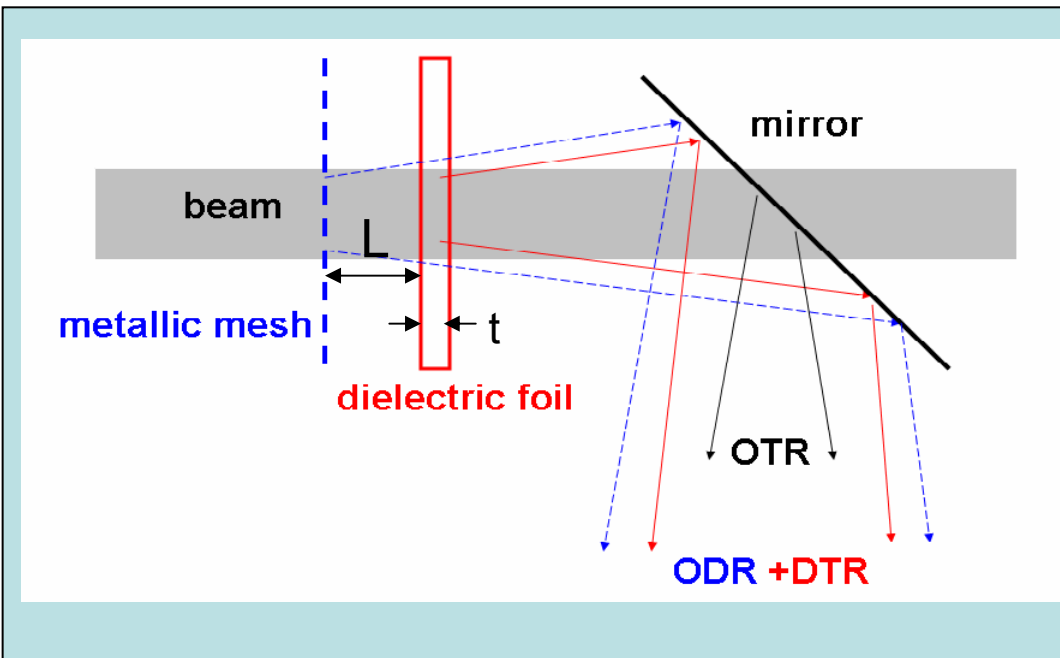


ODTRI

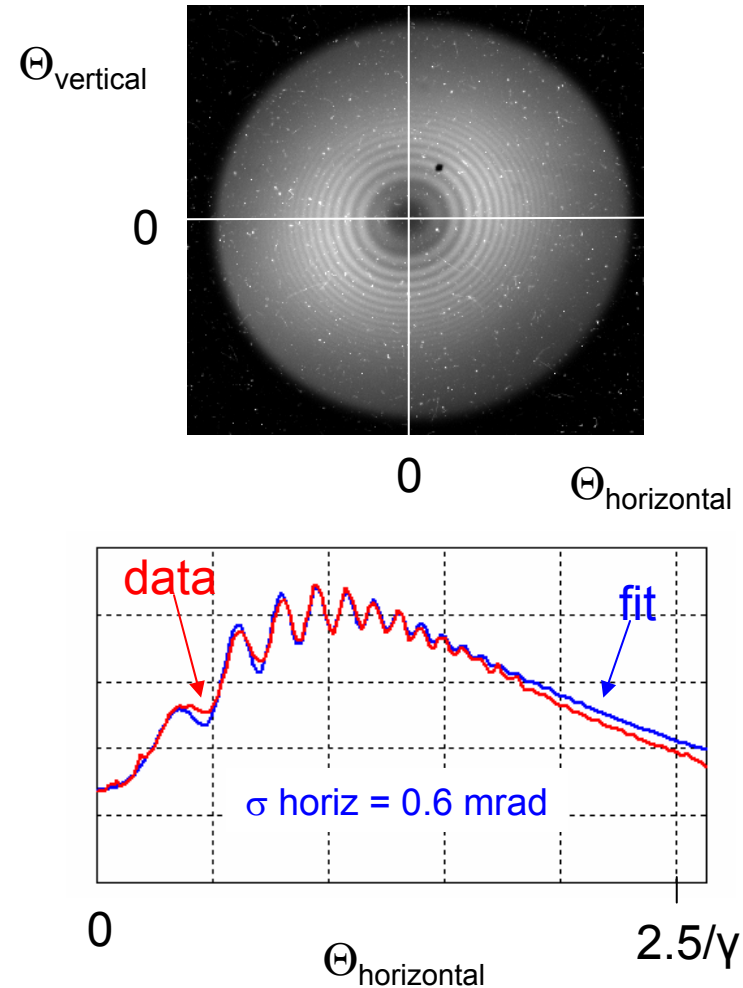


ODR-DTR Transmission Interferometer

Transmission interferometer needed at $E < 20$ MeV
(e.g. 8-15 MeV, $\gamma^2 \lambda \sim L = 1-10$ mm)

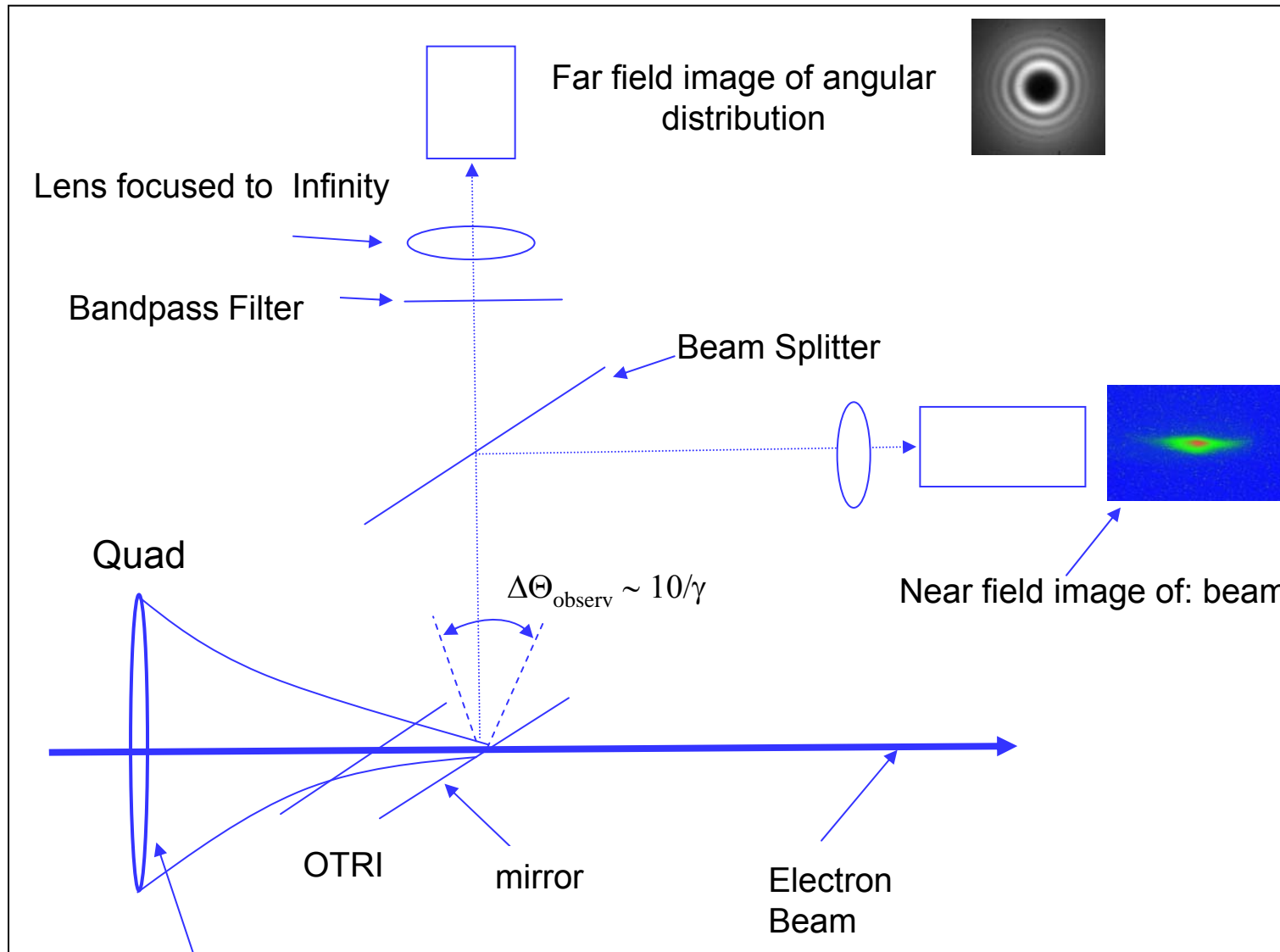


ANL/AWA: $E = 13.8$ MeV, $L = 3.7$ mm, $\lambda = 632$ nm, Kapton foil: $t = 9.15\mu$, index = 1.8



RMS Emittance Measurement using Near and Farfield Incoherent OTR

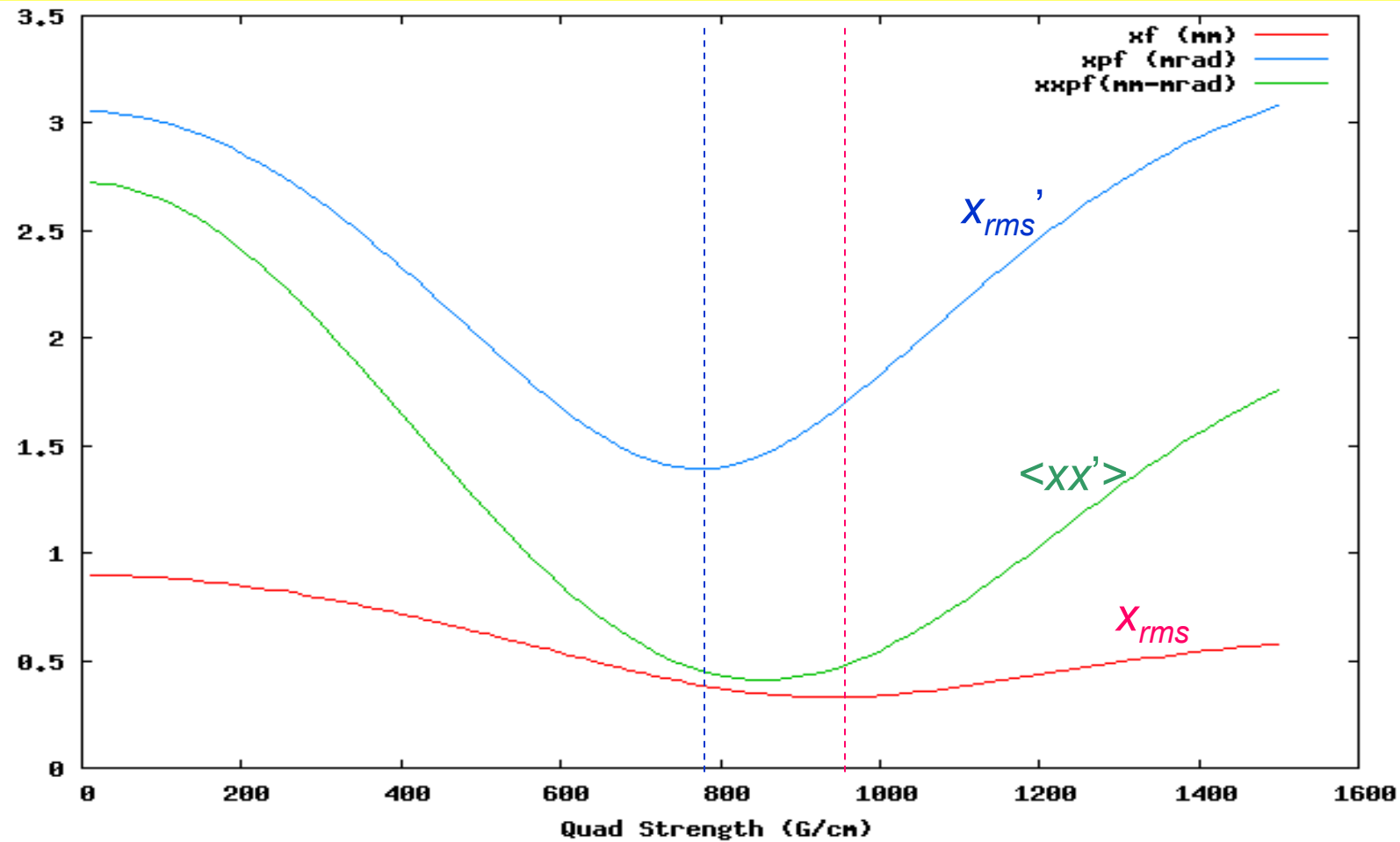
$$\tilde{\varepsilon}_x^2 = \langle x^2 \rangle \langle x'^2 \rangle - \langle xx' \rangle^2$$



At or near a beam waist, (e.g. x waist):

$$\langle xx' \rangle \approx 0 \quad \tilde{\varepsilon}_x^2 = \langle x^2 \rangle \langle x'^2 \rangle$$

Quadrupole Scan General Case: the minimum of the spot size or
minimum of the divergence is not close to a zero of the correlation term
(Emittance = 4.5 micron, Energy = 7.4 MeV)



New theoretical analysis allows more precise emittance measurement using OTR observables (x, x') *

Idea: The beam size $x(s, f)$ and the beam divergence $x'(s, f)$ have different minima w.r.t. to s, f . For each minimum we get a different value for the beam size-divergence correlation but the same rms emittance:

$$\epsilon_x^2 = \langle x^2 \rangle \langle x'^2 \rangle - \langle xx' \rangle^2$$

1) true beam waist:

difficult to achieve,
i.e. need to move foil along s
at a constant focusing strength f

$$\frac{\partial(x(f, s))}{\partial s} \Big|_{f=f_0} = 0 \rightarrow \langle x_w x' \rangle = 0$$

2) beam spot minimum:

achievable with a usual quad scan, i.e. vary f and minimize beam image observed with OTR

$$\frac{\partial(x(s, f))}{\partial f} \Big|_{s=L} = 0 \rightarrow \langle x_{\min} x' \rangle = \langle x_{\min}^2 \rangle / L$$

3) divergence minimum:

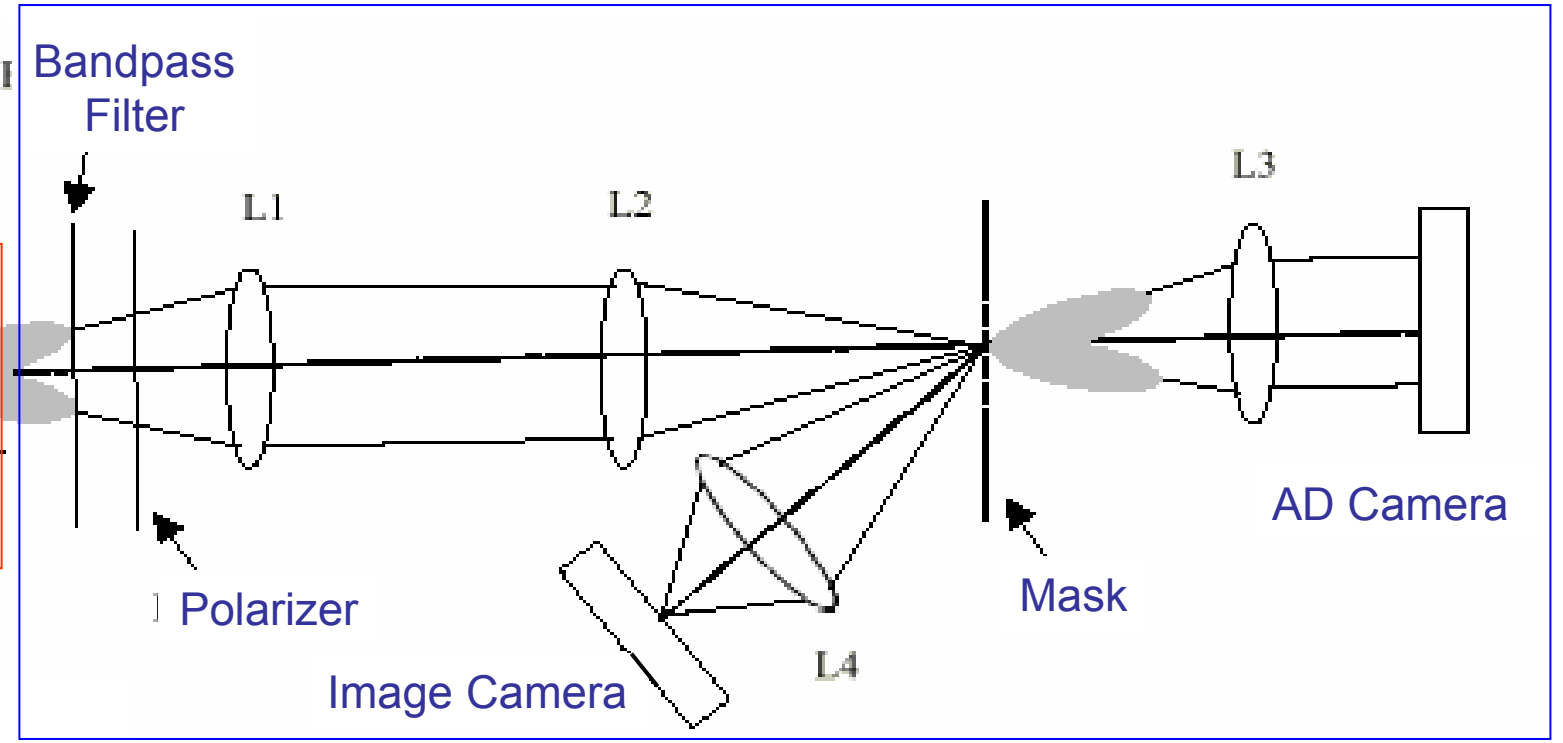
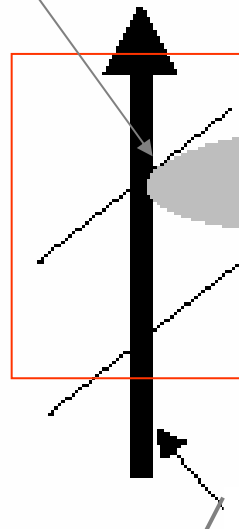
achievable by varying f to maximizing OTRI fringe visibility (angular quad scan)

$$\frac{\partial(x'(s, f))}{\partial f} \Big|_{s=L} = 0 \rightarrow \langle xx'_{\min} \rangle = L \langle x_{\min}^2 \rangle$$

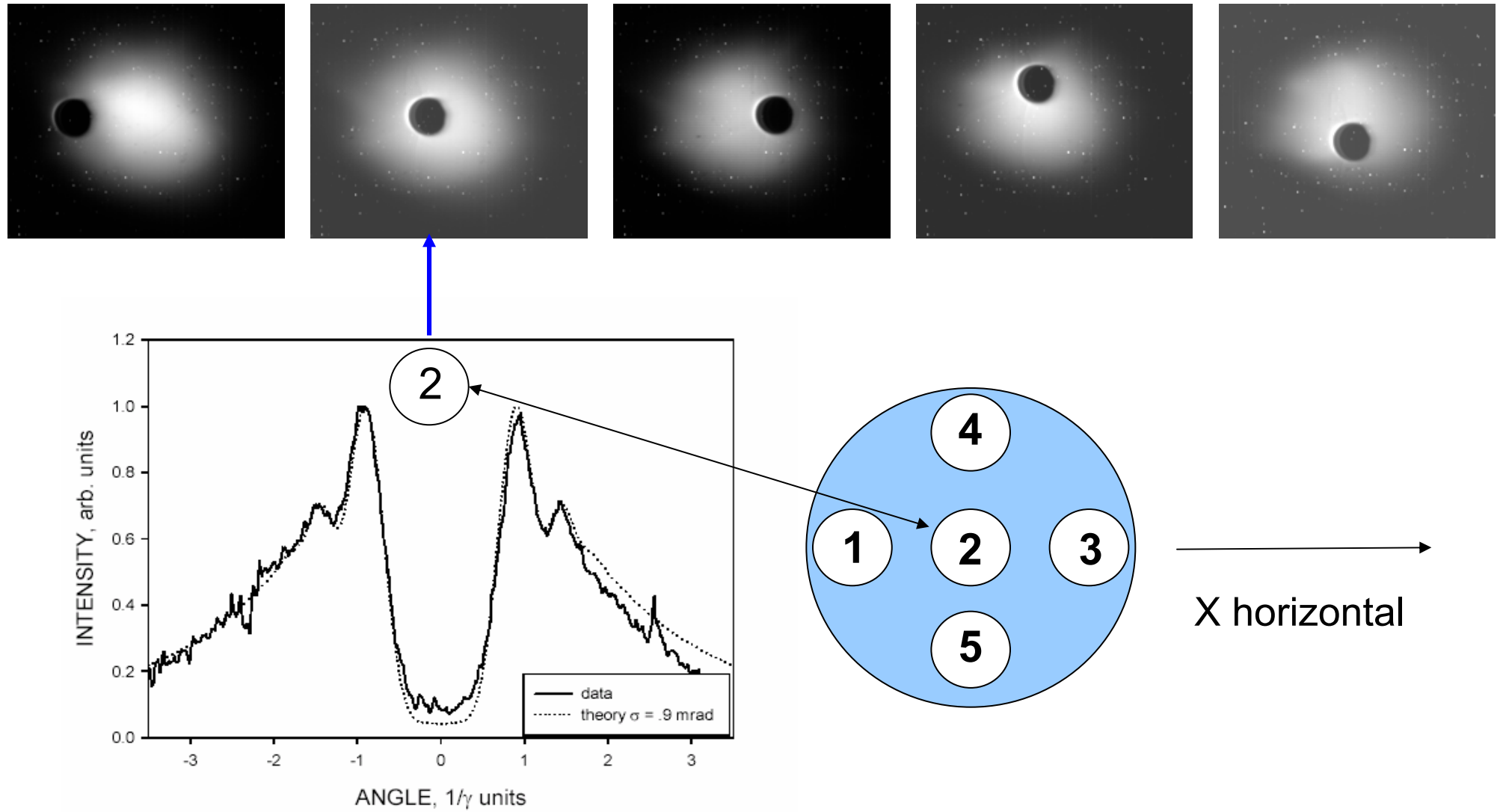
*(see Poster TH6REP053 for details)

Optical Phase Space Mapping: localized divergence and trajectory angle measured within beam image

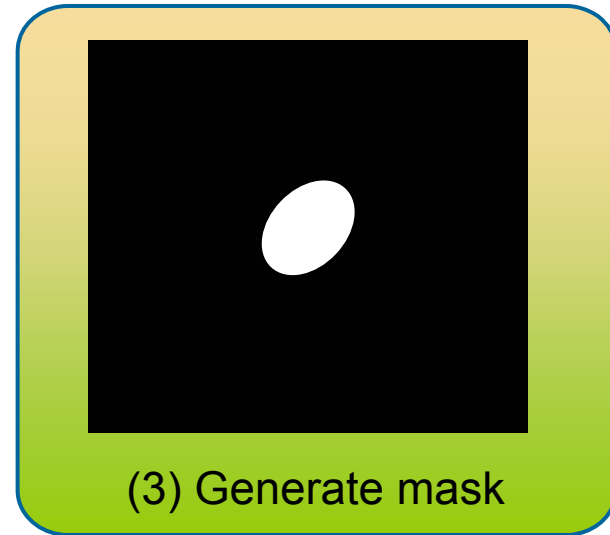
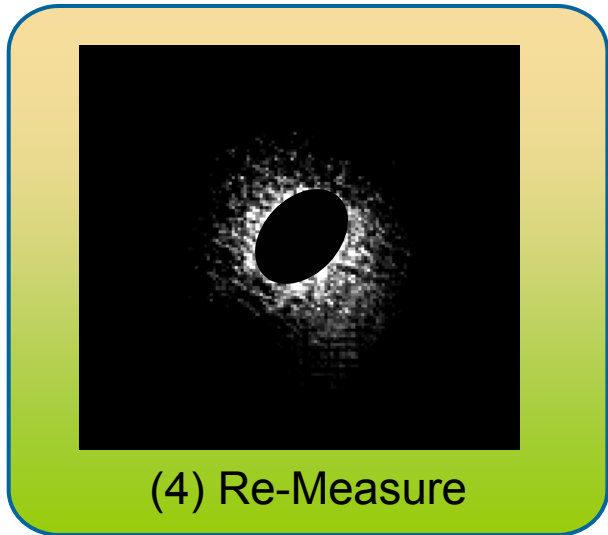
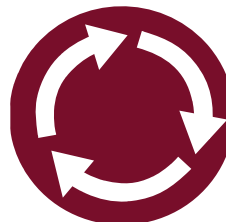
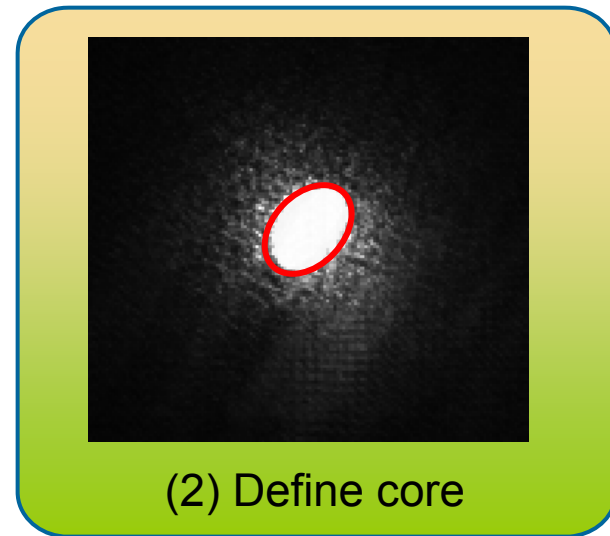
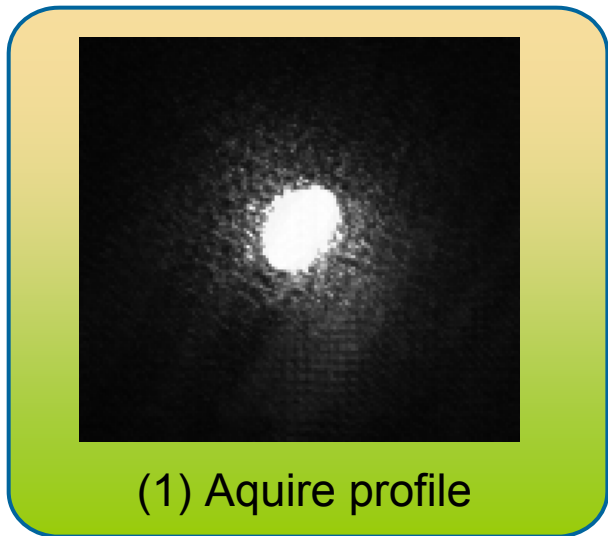
Optical
Radiation
(e.g. OTRI or
OSRI)



Localized (inter beam) OTRI divergence and trajectory Angle measurements using a 1mm pinhole (optical mask)



Proposed Study of Halo's using Dynamic Masking using Digital Micromirror Array (DMA)



Bunch Length Diagnostic using Radiation Fluctuation Analysis

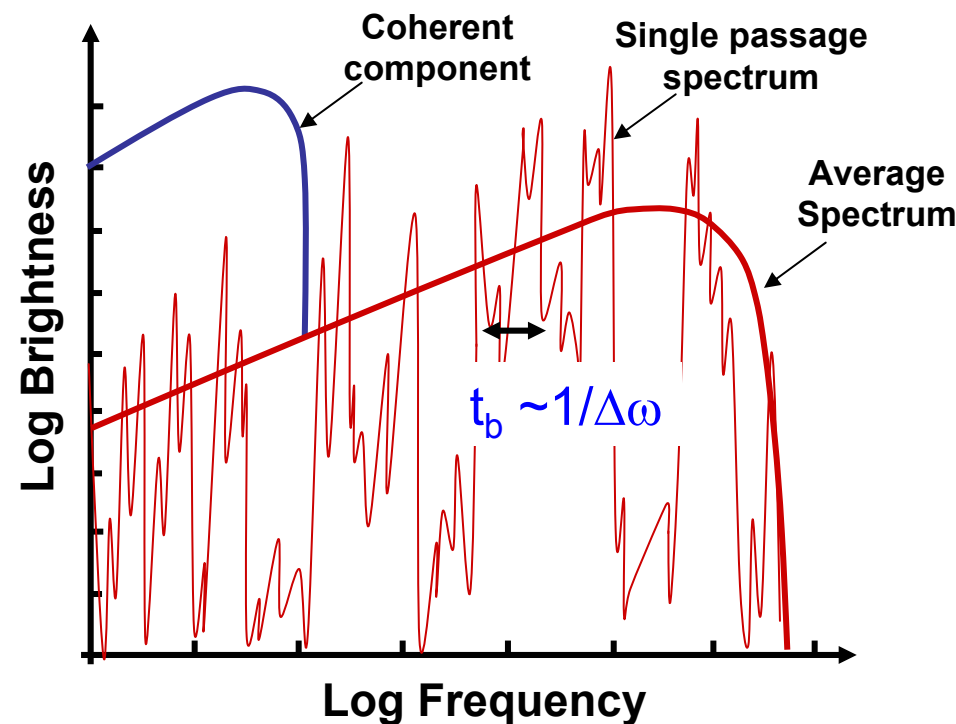


In real beams, due to presence of random modulation in the particle distribution, and to the variation of this modulation passage to passage, incoherent radiation is emitted with fluctuating intensity

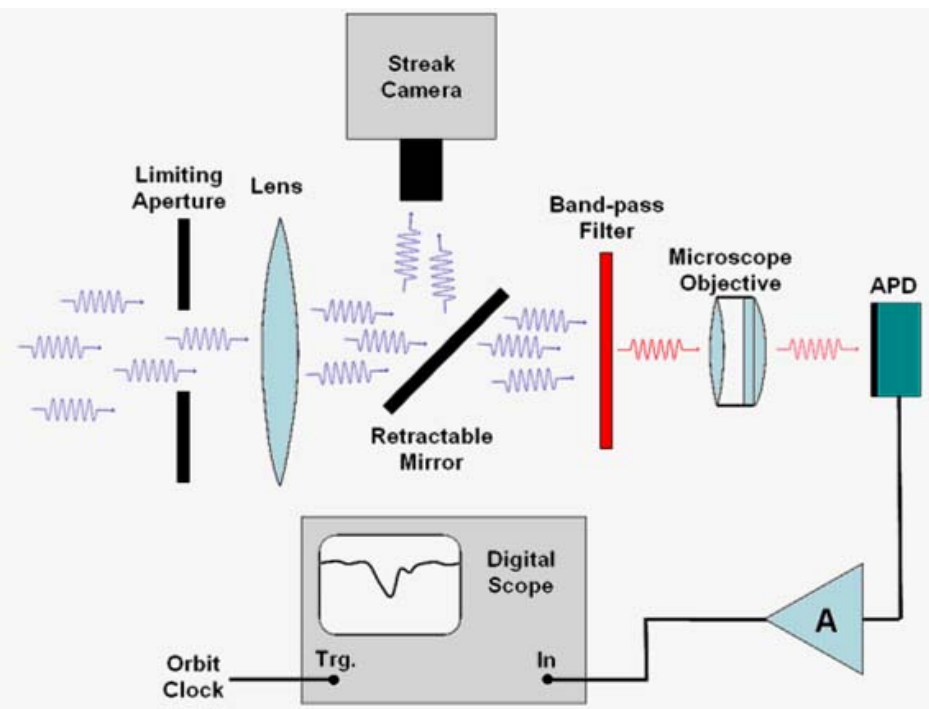
Stupakov, Zolotorev SLAC-PUB 7132, 1996) showed that the variance of the fluctuating radiation intensity incoh. part of spectrum can be used to measure bunch length.

Note 1: can be used with any kind of radiating process (OSR, OTR, etc.)

Note 2: that coherent component also has fluctuations which typically are not measurable (rel. amplitudes orders of magnitude smaller incoherent case) but in case of COTR due to chaotic microbunching they are visible.

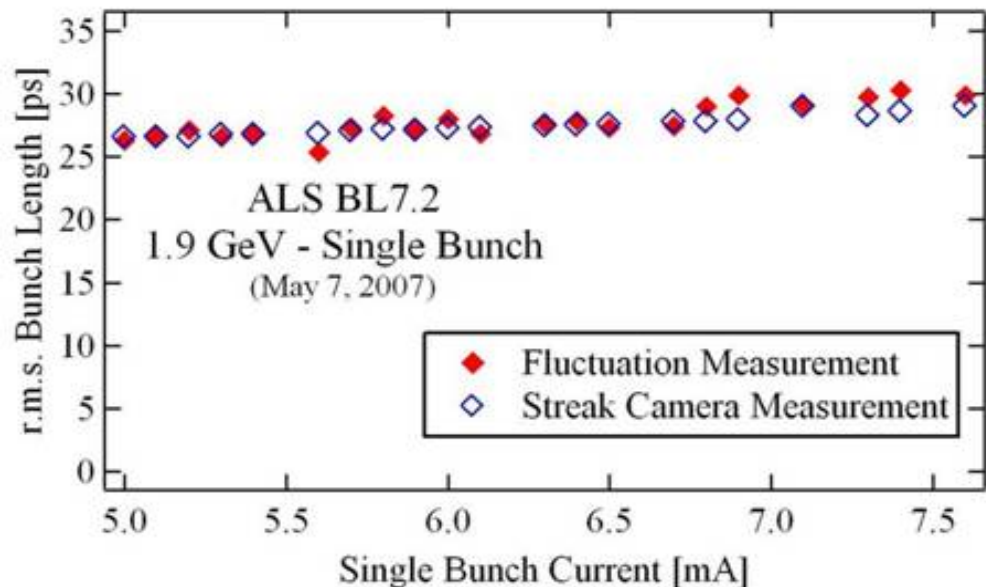


Absolute Bunch Length by IOSR Fluctuation Analysis at ALS



By using a bandpass filter with bandwidth σ_ω and measuring the passage to passage relative variance δ^2 of the radiation intensity, the bunch length σ_τ can be measured from:

$$\delta^2 = 1/\sqrt{1 + 4\sigma_\tau^2 \sigma_\omega^2}$$



Sannibale et al. PRST-AB 12, 032801 (2009).

COTR recently observed in e beams whose
and bunch lengths are much longer than optical wavelengths
(e.g. LCLS and FLASH at DESY)

Questions:

- Why is COTR observed in this situation?
- What are the spatial and angular distributions of the COTR?
- What is the spectrum of the radiation?
 - a. Is there enhanced COTR at given wavelengths?
 - b. Is the COTR resonant (i.e. the signature of periodic microbunching) or purely random in time (chaotic)
- Where in the beam profile is the COTR produced?
is it localized or random in space?
- COTR is a nonlinear function of N: bad for beam profiling;
- Can COTR be mitigated? how? spectral filtering? spatial filtering
- Can COTR be used as a diagnostic for underlying physics?

Coherent TR Radiation diagnostics

$$\frac{d^2I}{d\omega d\Omega} = \frac{d^2I_e}{d\omega d\Omega} \{N + N(N-1)f_{\perp}(k_{\perp}, \sigma_T)f_z(\sigma_z, k_z)\}$$

$$f_{\perp,z} = |F(\rho_{\perp,z})|^2$$

Degree of Coherency or Coherent Gain $G = I_{Coh} / I_{Incoh} = N f_{\wedge} f_z$

If transverse and longitudinal bunch distributions $\rho_{\perp,z}$ are Gaussian and $\theta \gg 1, k_{\wedge}; k_q$ and $k_z; k$

$$f_{\perp} = |F(\rho_{\perp})|^2 = \exp[-(\sigma_r k \theta)^2] \xrightarrow{\theta \gg 1/\gamma} \exp[-(\sigma_r / \gamma \lambda)^2] \xrightarrow{?} 1$$

$$f_z = |F(\rho_z)|^2 = \exp[-(\sigma_z k)^2] \approx \exp[-(\sigma_z / \lambda)^2] \xrightarrow{?} 1$$

image formed by the intensity of OTR fields from an entire bunch of N electrons is obtained from the superposition of the fields from each particle at locations r_j and z_j

$$\mathbf{E}_{S,N}(\mathbf{r}) = \sum_j e^{-ikz_j} \mathbf{E}_S(\mathbf{r} - \mathbf{r}_j)$$

$$|\mathbf{E}_{S,N}(\mathbf{r})|^2 = N \int d^2 r' dz \rho(\mathbf{r}', z) |\mathbf{E}_S(\mathbf{r} - \mathbf{r}')|^2 + N^2 \left| \int d^2 r' dz e^{-ikz} \rho(\mathbf{r}', z) \mathbf{E}_S(\mathbf{r} - \mathbf{r}') \right|^2$$

IOTR intensity: convol. of ρ with single particle INTENSITY on the foil

COTR Image: convolution of the particle distribution with single particle FIELD on the foil

Two regimes for COTR Imaging:

1) Beam size $\sigma < \gamma\lambda$

COTR Image is convolution of PSF with beam distribution, or in extreme case $\sigma \ll \gamma\lambda$, just the PSF

2) Beam size $\sigma > \gamma\lambda$

COTR Image is gradient of beam distribution

Loos, et. al. SLAC Pub 13395
and Proc. of FEL08

Henrik Loos

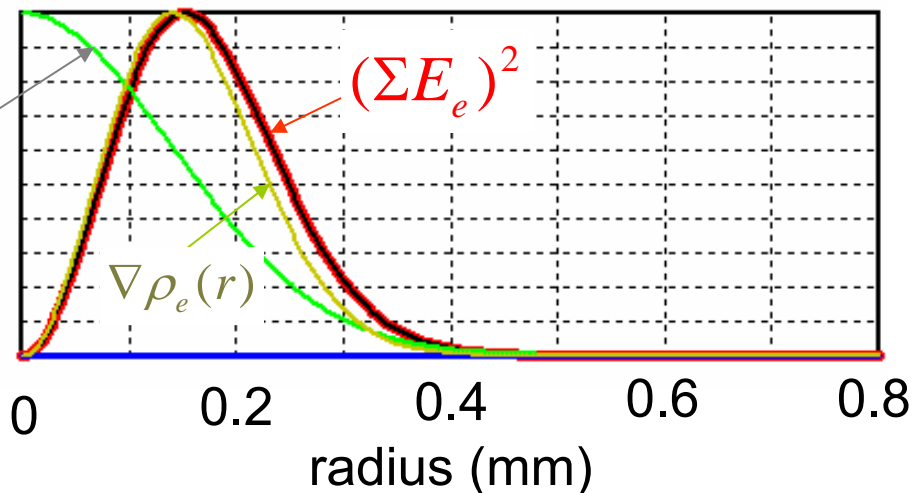
loos@slac.stanford.edu

Calculations of Near Field and Far field Intensity of COTR

250 MeV Gaussian beam ($\sigma = 0.2\text{mm} > \gamma\lambda/2\pi$)

Near Field Intensity of COTR

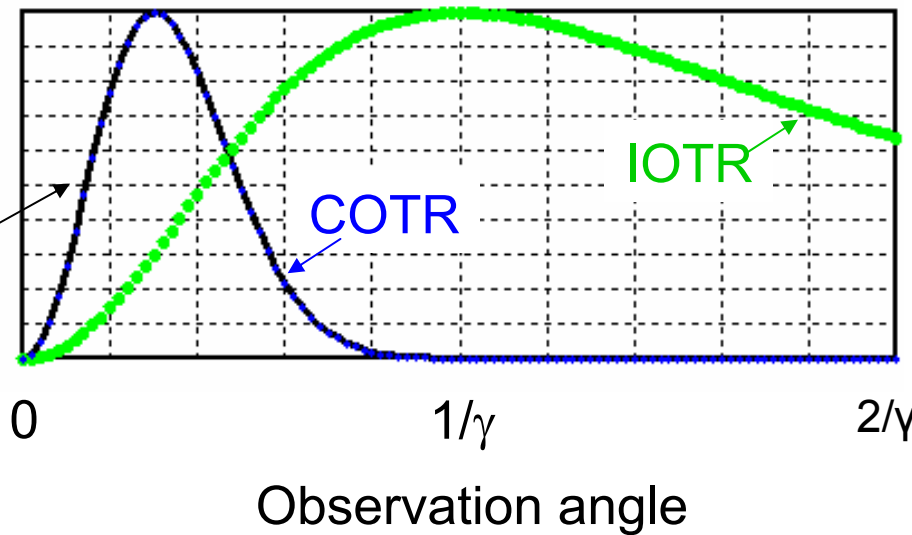
$$\rho_e(r) = \frac{1}{\pi\sigma} \exp(-r^2 / \sigma^2)$$



Far field (Angular) Intensities of COTR and IOTR

$$I_{COTR} = I_{IOTR} \cdot |f_\perp(k_\perp)|^2$$

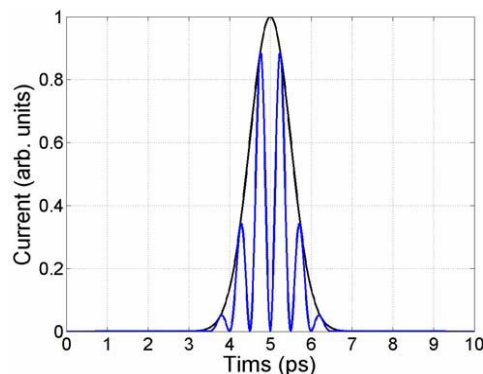
$$f_\perp(k_\perp) = \exp\left[-(\pi\sigma \sin \theta / \lambda)^2\right]$$



CTR from periodically micro-bunched beams

- Produces periodic modulations in longitudinal charge and form factor leading to appearance of lines in the CTR spectrum at the harmonics (nk_r) of the inter micro-bunch modulation frequency.
- Theory well developed by Rosenzweig, Travish and Remaine NIMA1995
- Experimentally studied in a number of experiments in the THz and optical regimes.

Periodically modulated beam

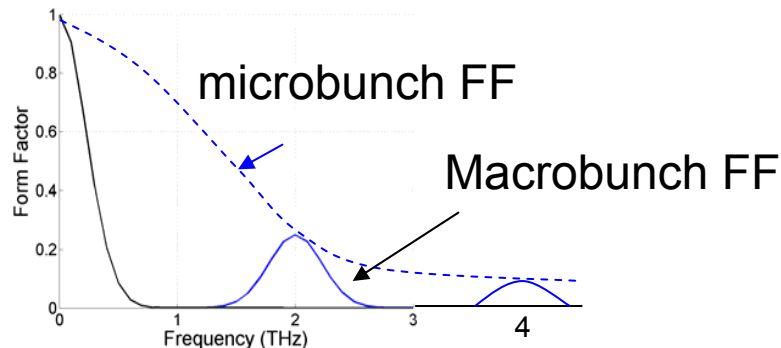


Model for Charge density

$$\rho(z) = \frac{\exp(-z^2 / 2\sigma_z^2)}{2\sqrt{\pi}\sigma_z} \left[1 + \sum_{n=1}^{\infty} b_n \cos(nk_r z) \right]$$

Longitudinal form factor:

$$F_L = \sum_{n=-\infty}^{\infty} b_n^2 \exp(-(k - k_r)^2 \sigma_z^2)$$



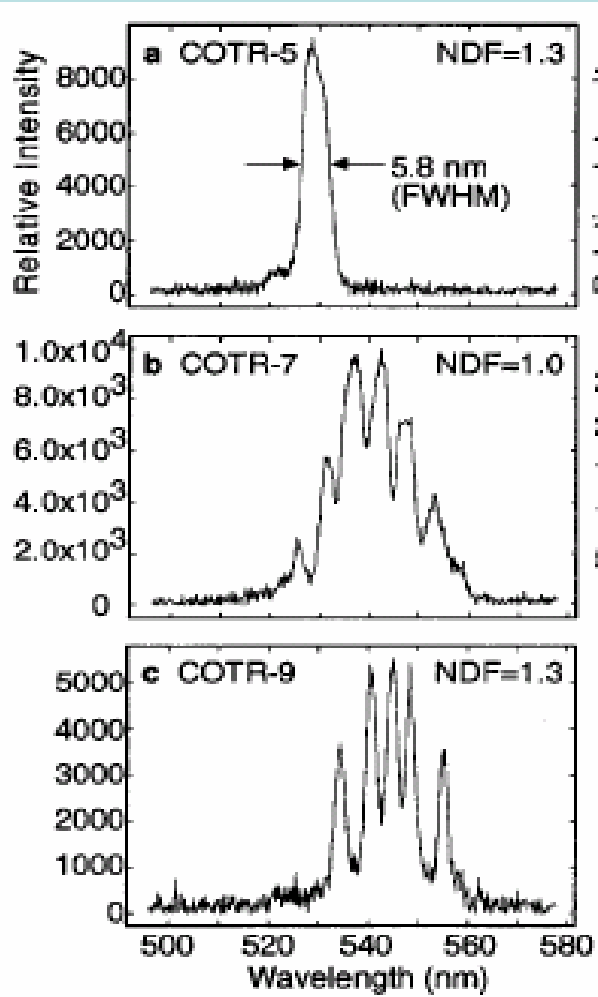
$P \ I_{CTR}^n \mu \ N b_n^2$

bunching fraction

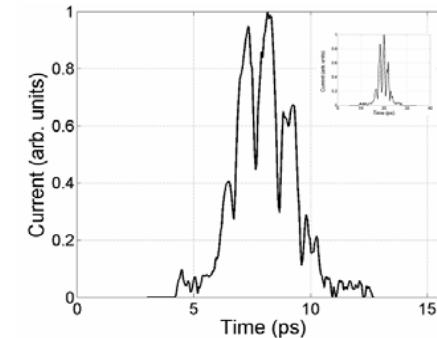
COTR Observations

CTR Spectral Observations showing Periodic Microbunching

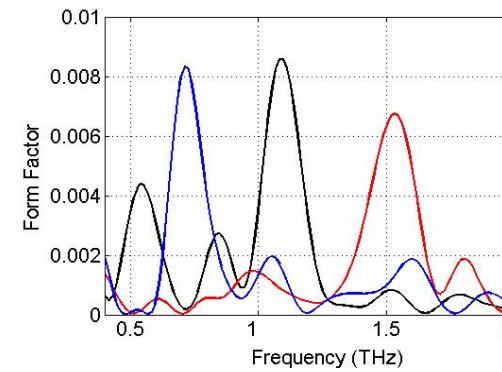
Development of COTR Sidebands in a SASE FEL: exponential gain regime to saturation
(A.Lumpkin,et. al. PRL 2002)



CTTR previously observed in THz laser photo cathode modulation experiments at BNL-SDL
(J.Neumann et. al. J.Appl.Phys. 2009)



Longitudinal profile of e beam ($Q=20\text{pc}$)



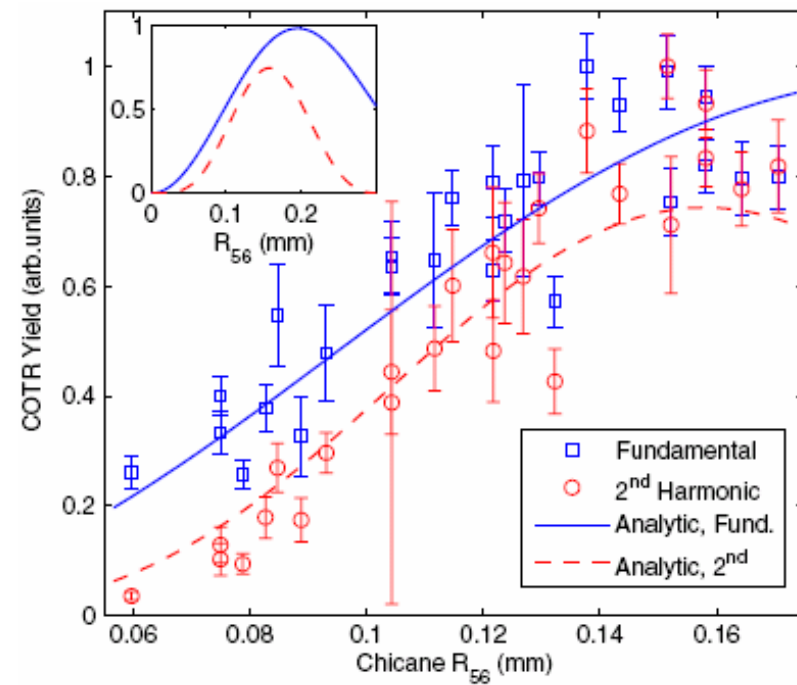
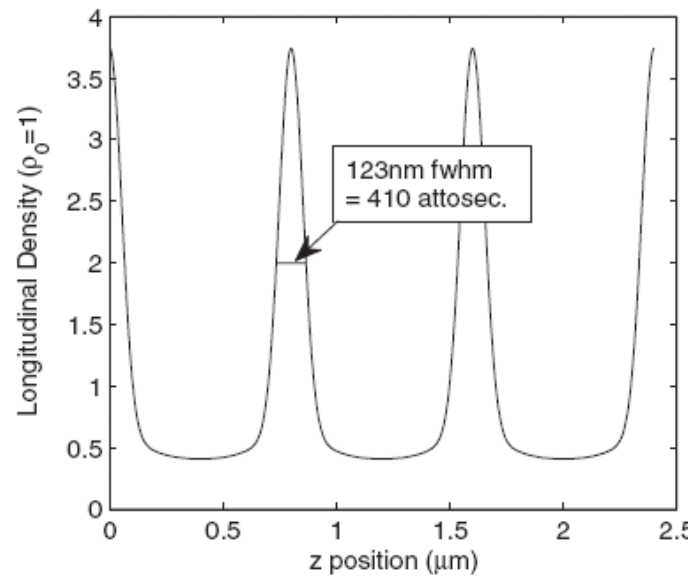
Longitudinal Form factor for different microbunch modulation frequencies

COTR from energy modulated IFEL passing through a chicane*

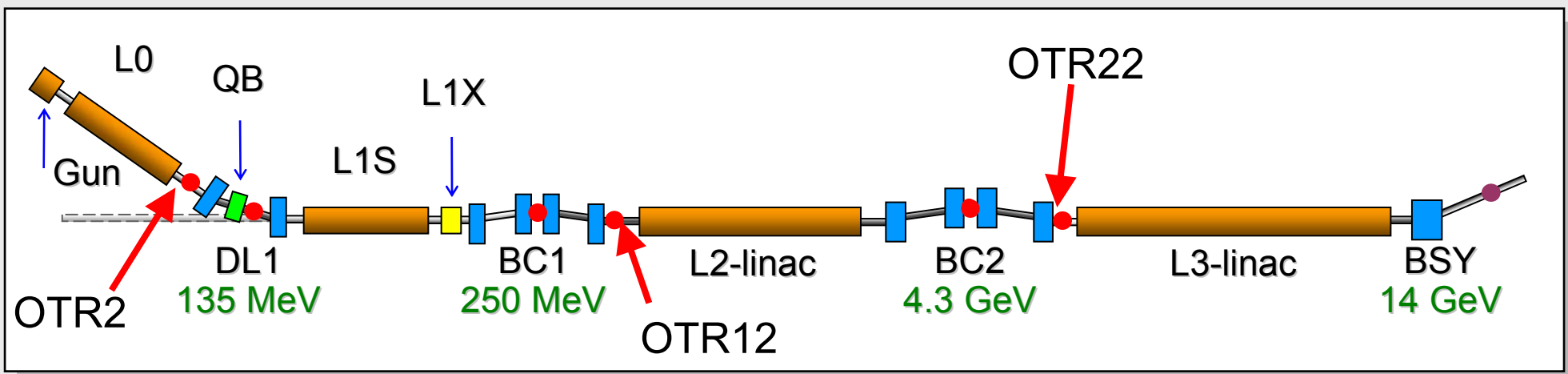
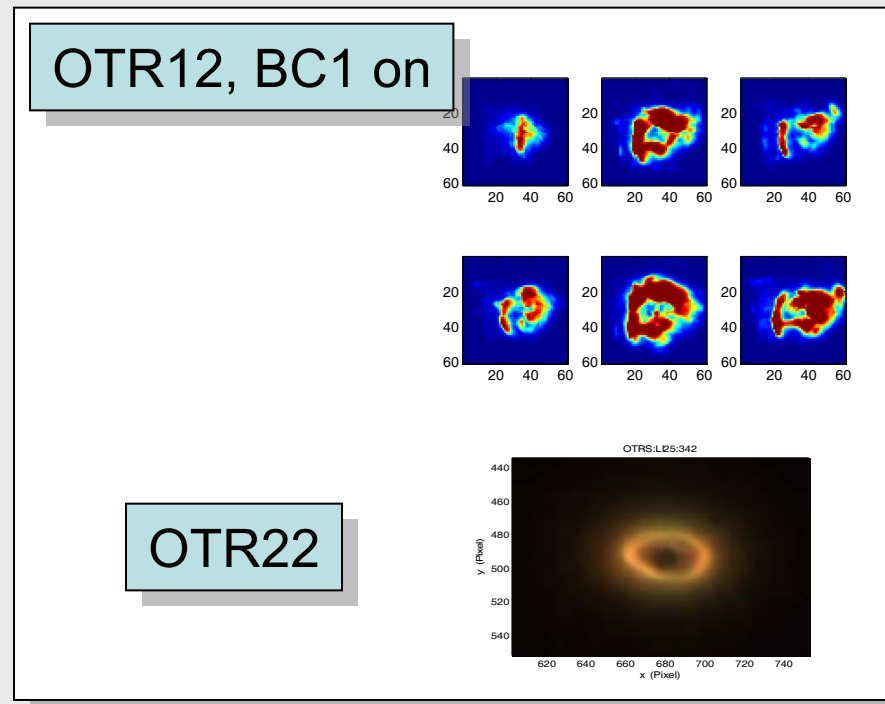
IFEL energy modulation

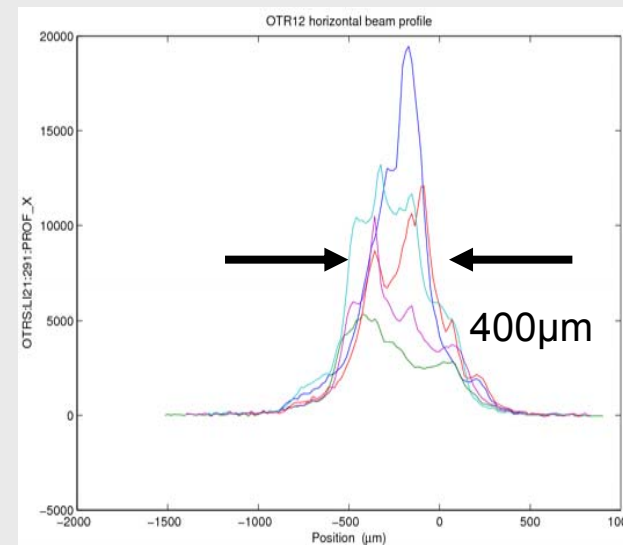
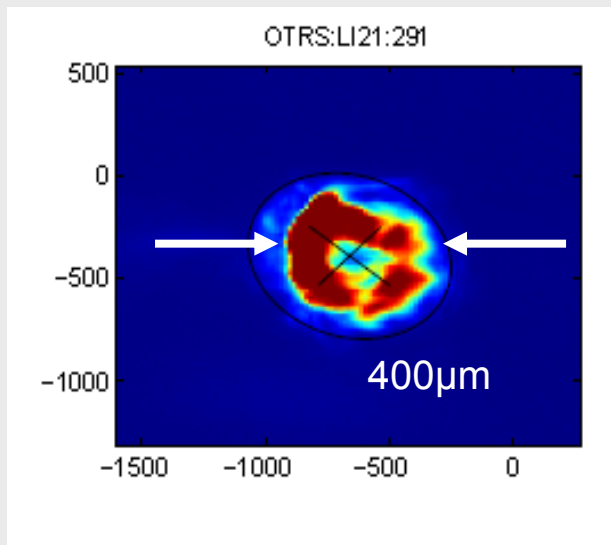
$$g = g_0 + h \sin(k_l z_0)$$

$$I_{\text{COTR}}^n \mu b_n^2 = [J_n(nk_l R_{56} \eta)]^2 \exp \left[-\left(\frac{nk_l R_{56} \sigma_y}{\gamma_0} \right)^2 \right].$$



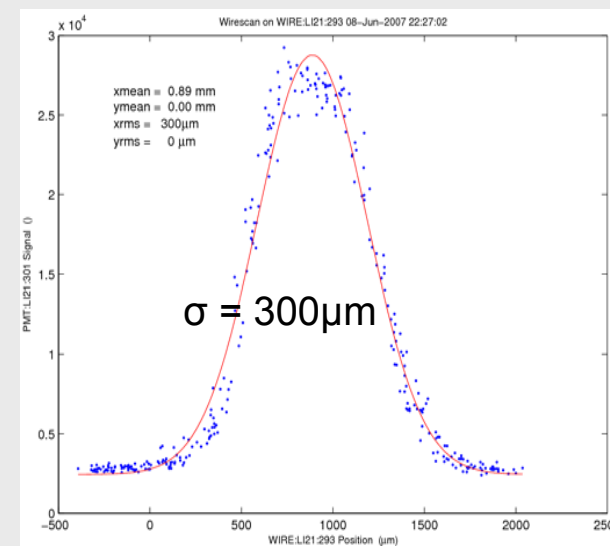
- OTR2: Light linear with charge
- OTR12, BC1 off: Enhanced by ~4-6, beam size changes
- OTR12, BC1 on: Enhanced by <100, transverse structure
- OTR22, BC1&2 on: Enhanced by <10⁵, break up, rings

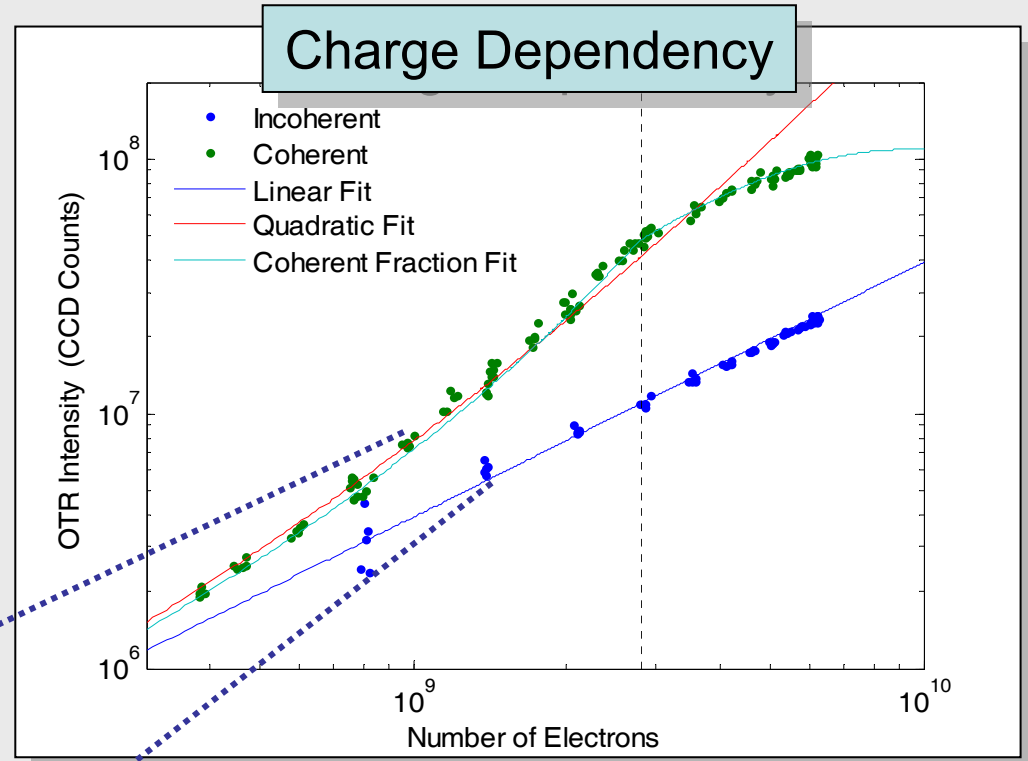
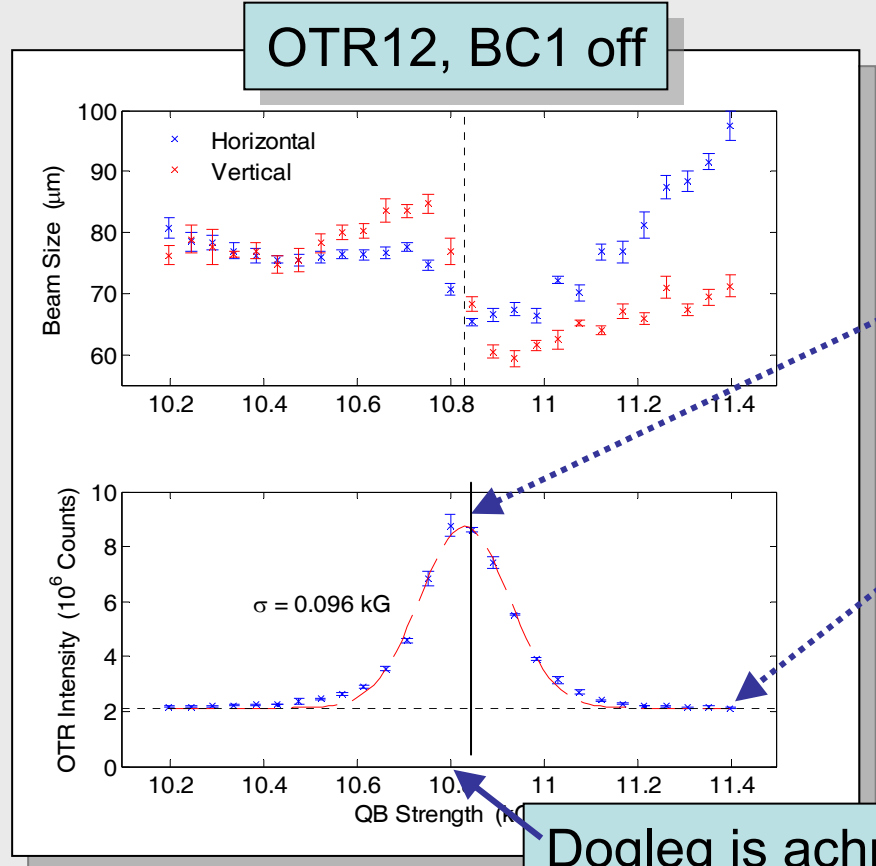
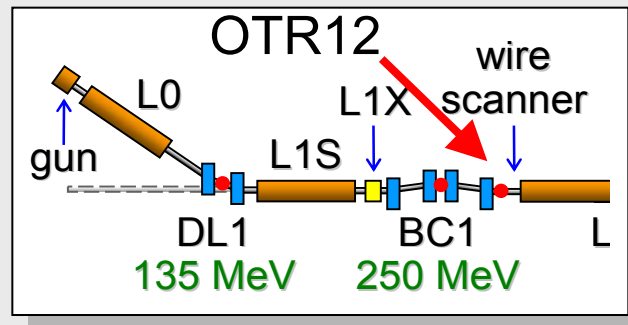




LSC microbunch Instability:

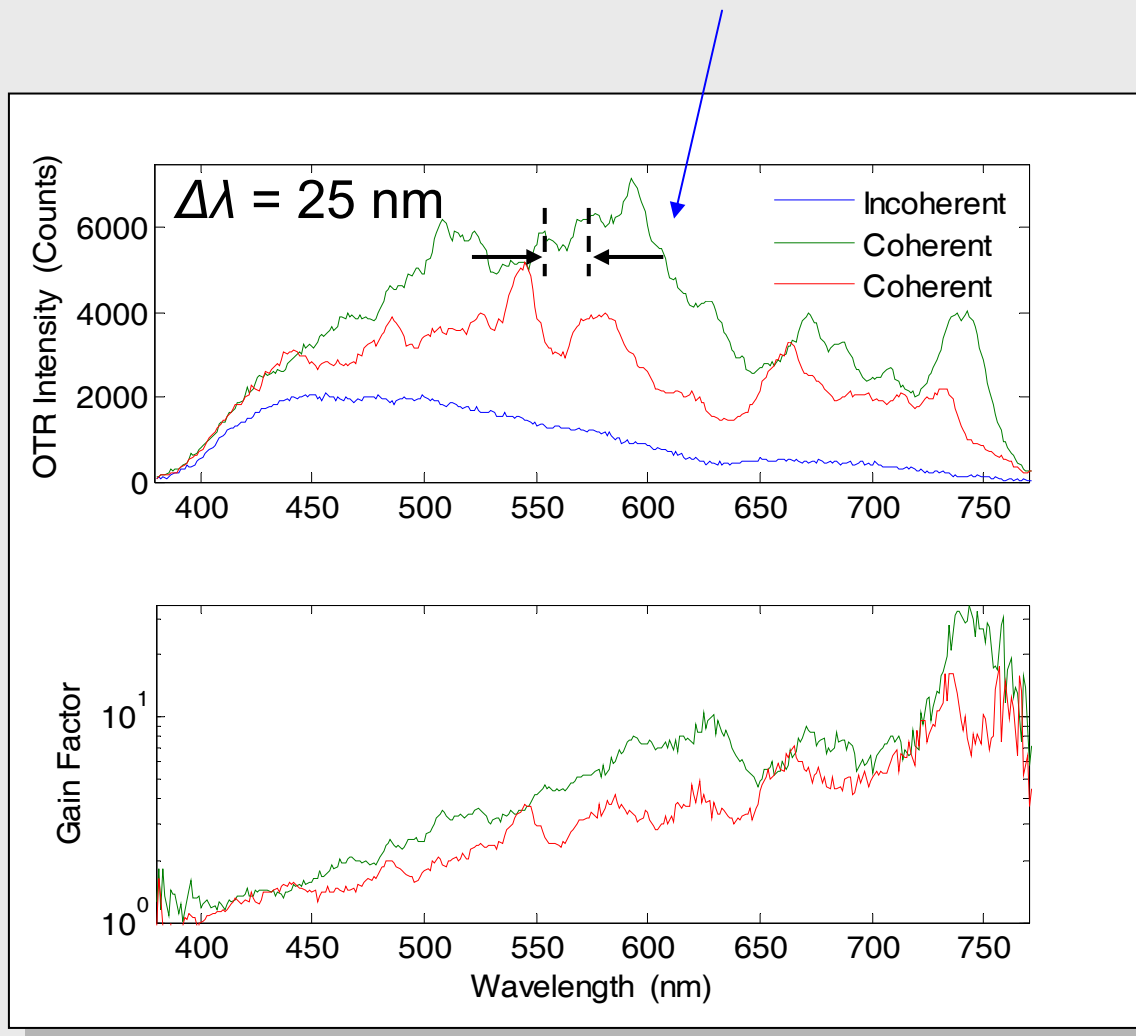
- 1) shot noise: longitudinal density fluctuations produce energy modulations
- 2) energy modulations convert to increased density modulation by R_{56} in DL1 (or in bunch compressor sections)





Dogleg is achromat: preserves microbunching

Shot to shot optical fluctuations ($\lambda \ll c\tau_b = 60 \mu\text{m}$) ; $|I| > |I_{\text{incoherent}}$

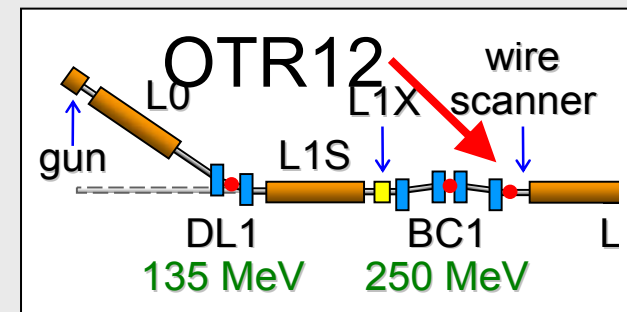


Measure COTR spectrum with CCD and transmission grating

OTR12 at normal Compression
60 μm bunch length

Spike width resolution limited

COTR gain increases exponentially from blue to red



Theoretical Microbunching Instability Gain Curves compared to Data

Gain

bunching fraction

$$G(k, R_{56}, g_0, dE_0, s_{x0}, \dots) = |b(k)|^2$$

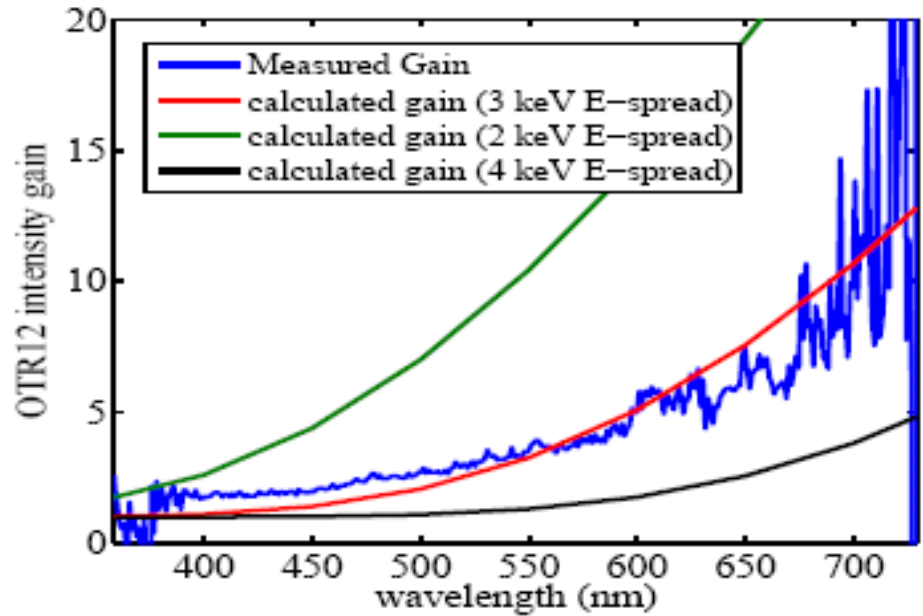
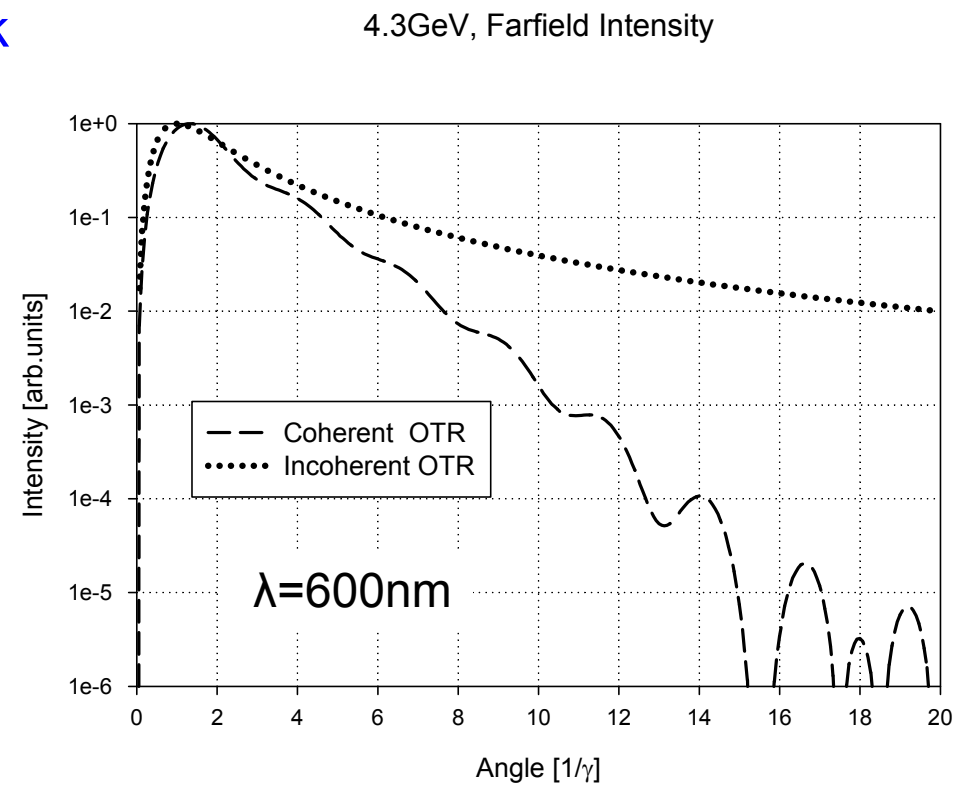
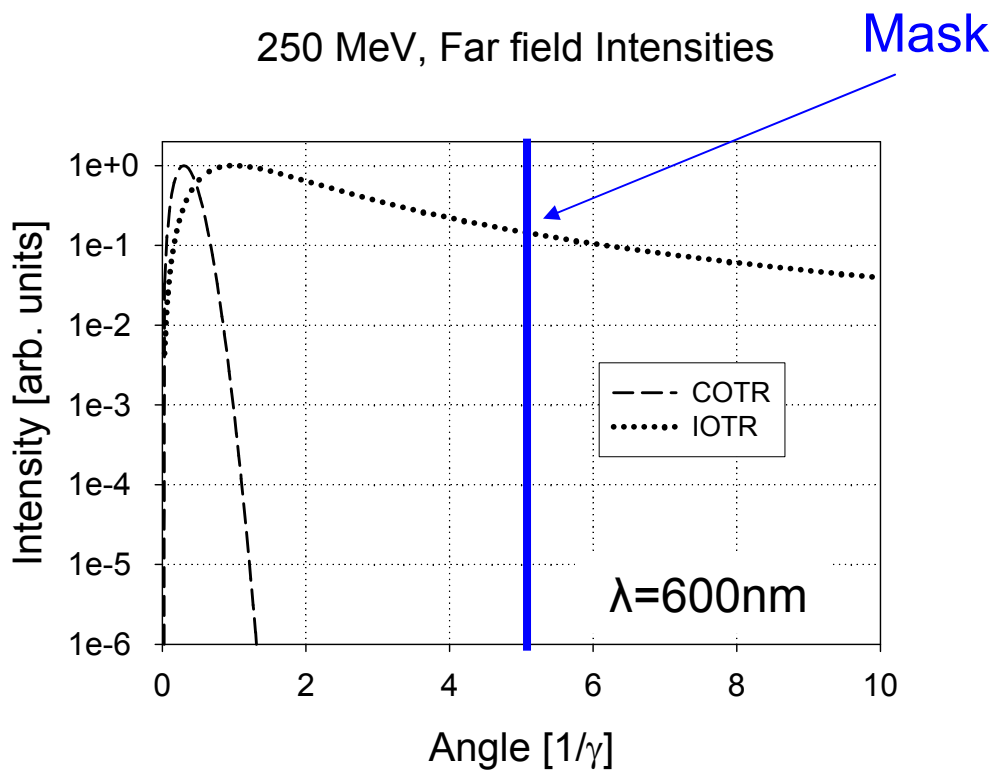


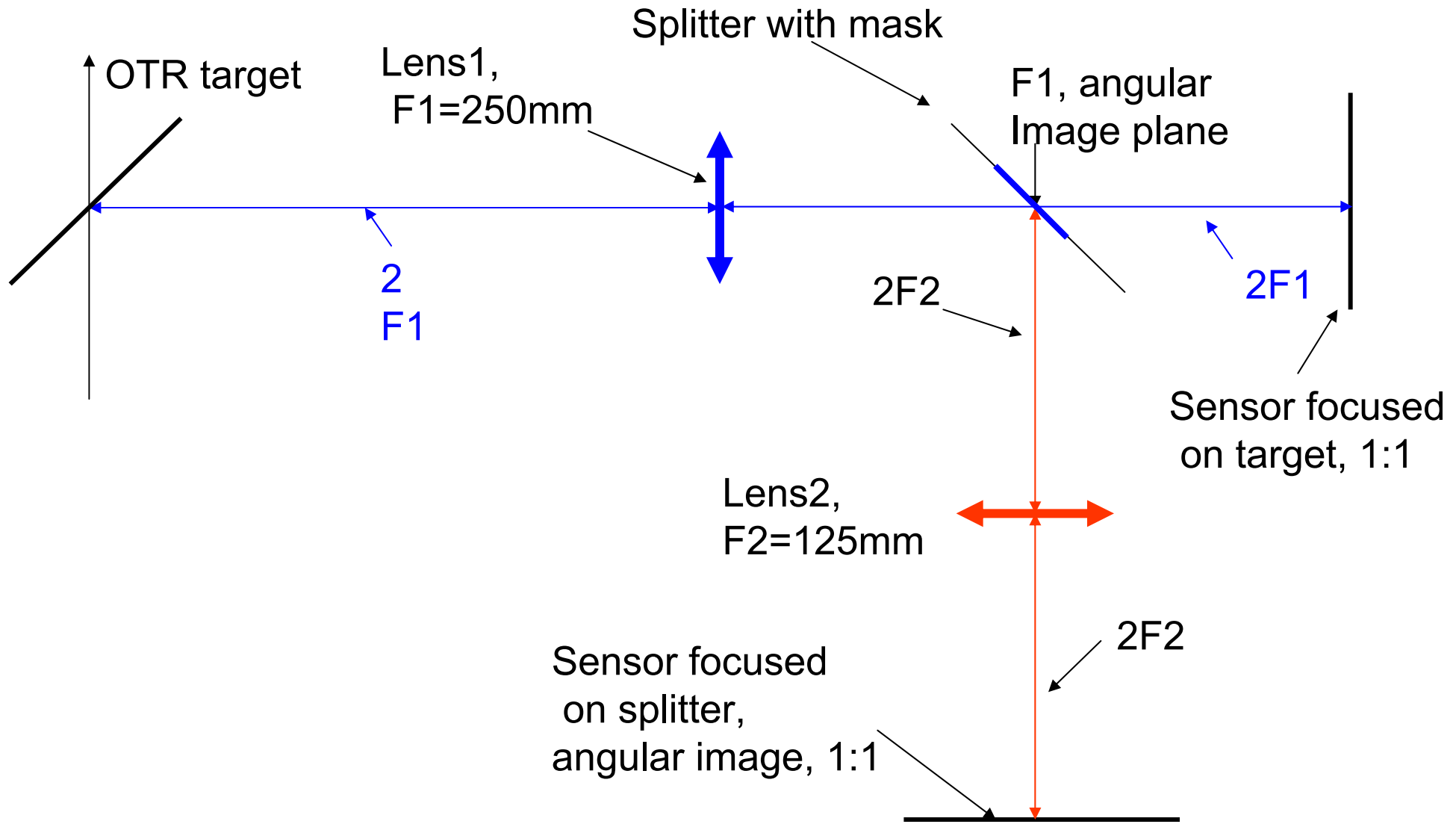
Figure 3: Measured and calculated OTR intensity gain for 250 pC charge at OTR12 as a function of the optical wavelength. $E = 250$ MeV, $\sigma = 0.2$ mm

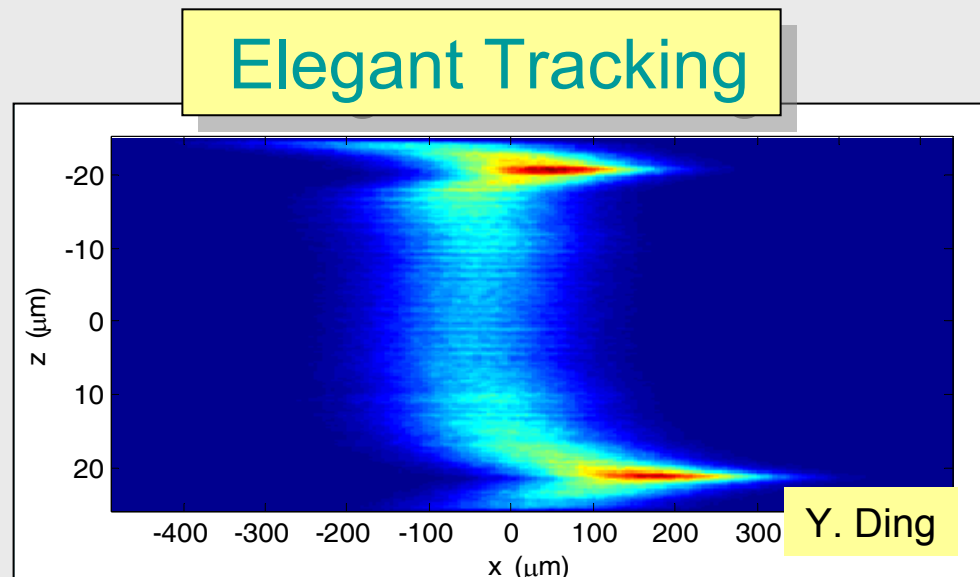
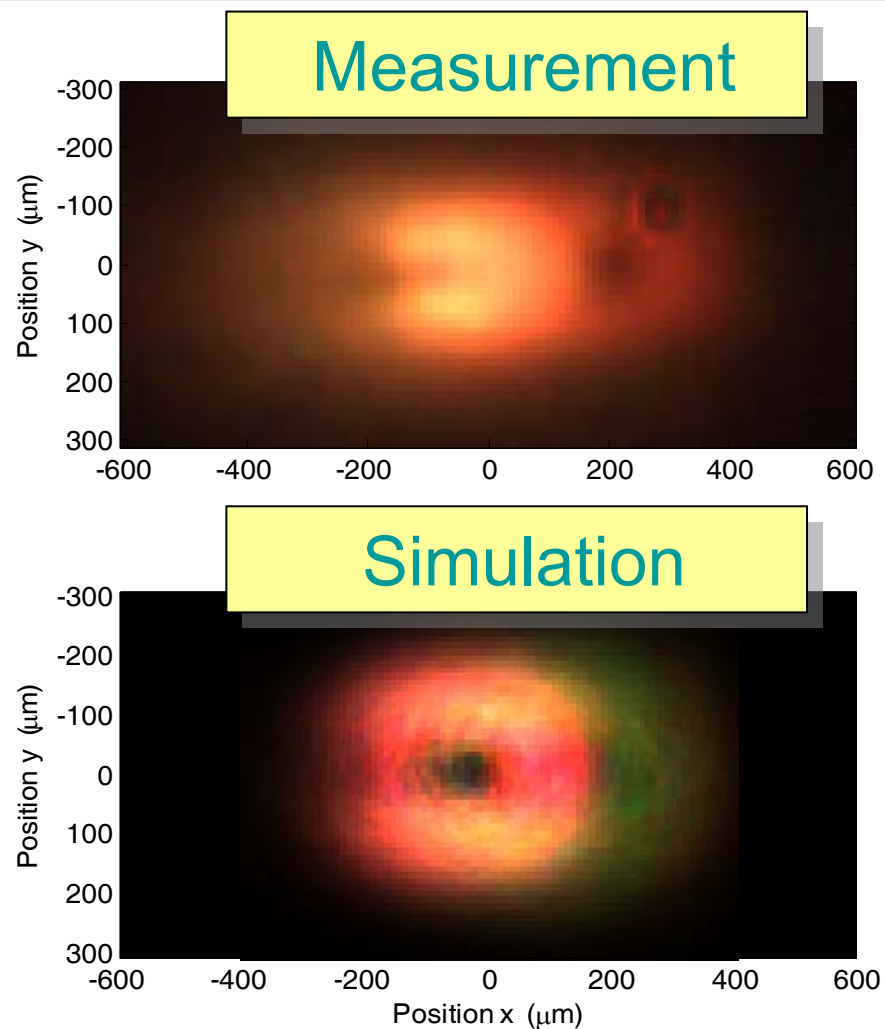
Mitigation of COTR* by Fourier Plane Spatial Filtering



* See also PAC09 Poster Papers: TH5RFP043, TH6REP021

Optical system for spatial filtering/mitigation of COTR





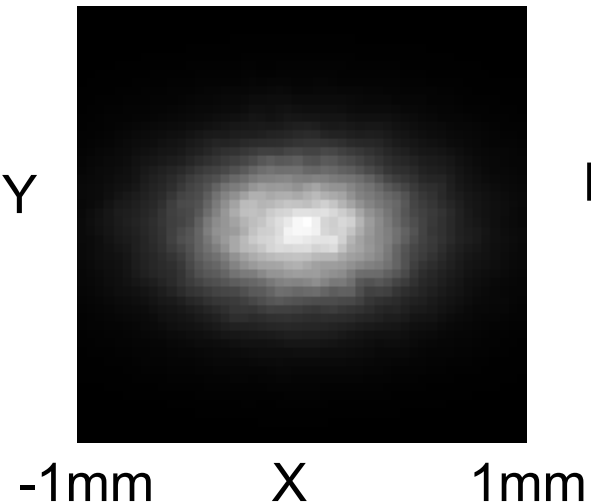
Use Elegant tracking data at OTR22 for 2% initial modulation at 40 μm

COTR simulation calculates form factor transversely resolved for 11 λ 's

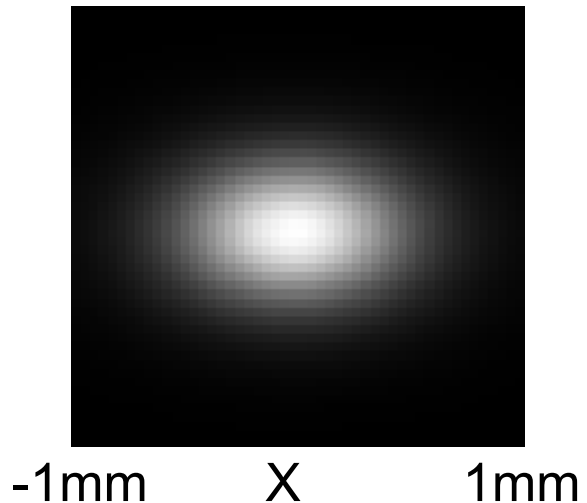
Indication that the two rings are from current peaks in bunch at head & tail

Simulation Code predicts IOTR and COTR distributions using ELEGANT
FERMI@Trieste, Linac1 (250 MeV), $\Delta\lambda=0.5\text{-}1.0\mu\text{m}$

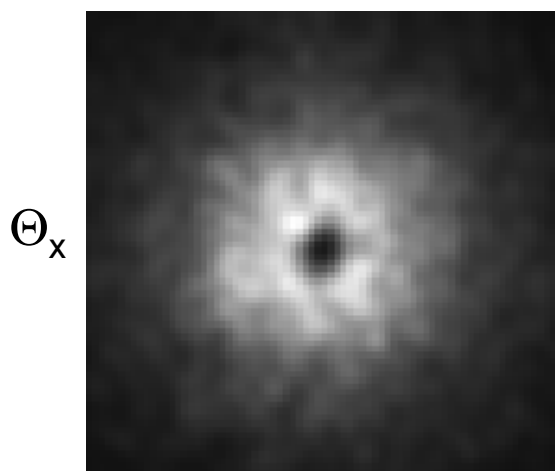
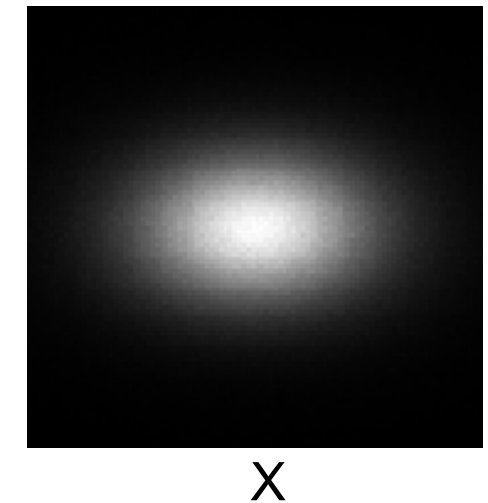
coherent $I_{\max}=1.34\text{E}9$



incoherent $I_{\max}=1.26\text{E}9$



Particle distribution

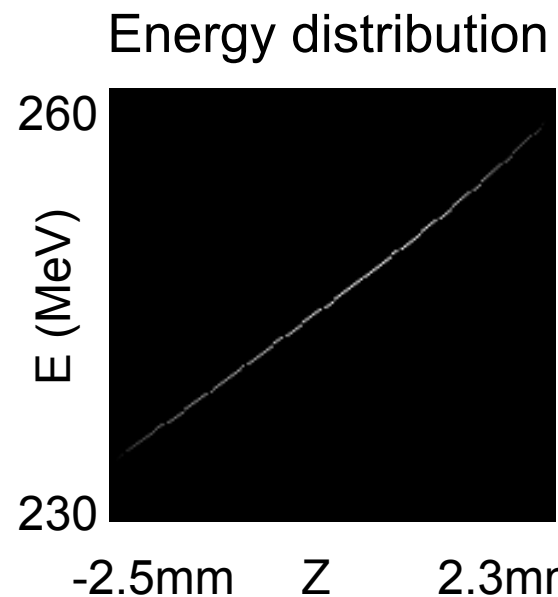


Far field
(ang.distrib.)

coherent $I_{\max}=3.84\text{E}12$



incoherent $I_{\max}=3.16\text{E}12$

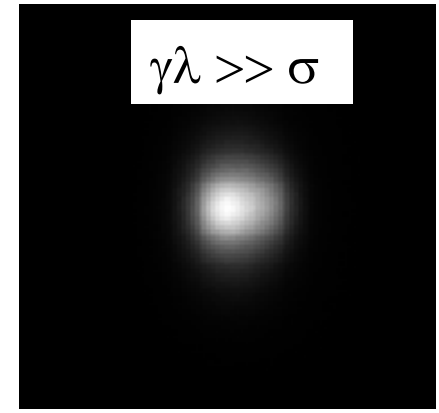
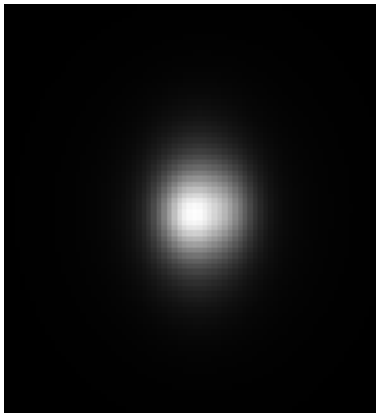
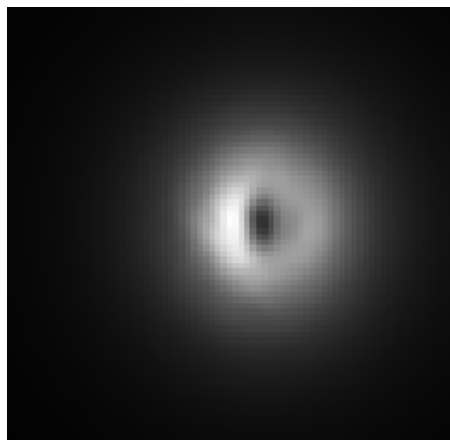


Energy distribution

IIRTR and CIRTR expected from FERMI@Trieste after 2nd bunch compressor linac 4

(E= 1.2 GeV, $\Delta\lambda = 2\text{-}4\mu\text{m}$, $\gamma\lambda \gg \sigma$)

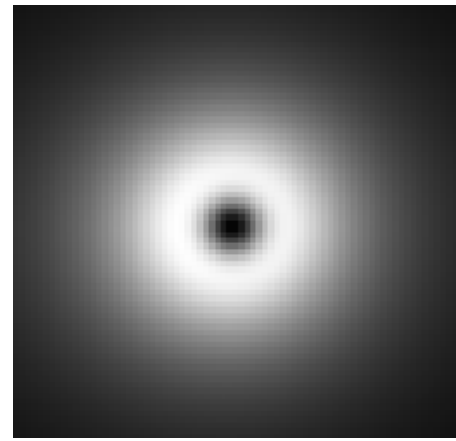
bunch distribution



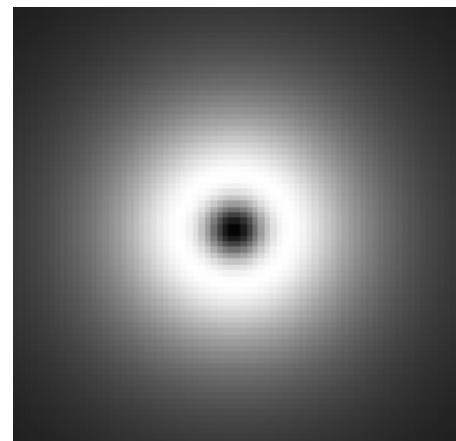
coherent I_{max}=6.46E10

Incoherent I_{max}=5.94E9

-0.75mm X 0.75mm



-4 $\Theta(1/\gamma)$ 4



Coherent I_{max}=3.6E15

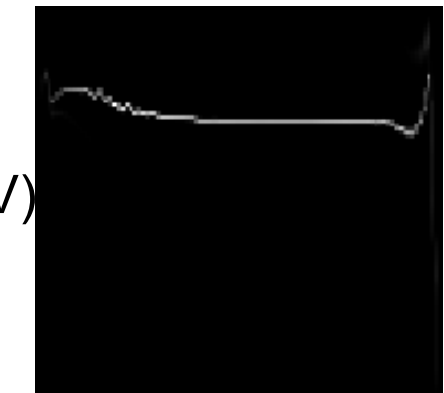
Incoherent I_{max}=3E13

energy distribution

1208

E(MeV)

1180



-0.14mm Z 0.15mm